Tectonophysics 609 (2013) 690–705

Contents lists available at ScienceDirect

Tectonophysics

journal homepage: www.elsevier.com/locate/tecto

Review Article

The character of the Moho and lower crust within Archean cratons and the tectonic implications

Dallas H. Abbott [a,*], Walter D. Mooney [b], Jill A. VanTongeren [c]

[a] Lamont–Doherty Earth Observatory of Columbia University, Palisades, NY 10964
[b] US Geological Survey, Menlo Park, CA 94025
[c] Rutgers University, Piscataway, NJ 08854

ARTICLE INFO

Article history:
Received 7 April 2013
Received in revised form 2 September 2013
Accepted 10 September 2013
Available online 18 September 2013

Keywords:
Archean
Moho
Seismic
Granite
Greenstone belt
Crust

ABSTRACT

Undisturbed mid Archean crust (stabilized by 3.0–2.9 Ga) has several characteristics that distinguish it from post Archean crust. Undisturbed mid-Archean crust has a low proportion of internal seismic boundaries (as evidenced by converted phases in seismic receiver functions), lacks high seismic velocities in the lower crust and has a sharp, flat Moho. Most of the seismic data on mid-Archean crust comes from the undisturbed portions of the Kaapvaal and Zimbabwe (Tokwe segment) cratons. Around 67–74% of younger Archean crust (stabilized by 2.8–2.5 Ga) has a sharp, flat Moho. Much of the crust with a sharp, flat Moho also lacks strong internal seismic boundaries, but there is not a one to one correspondence. In cases where its age is known, basaltic lower crust in Archean terranes is often but not always the result of post Archean underplating. Undisturbed mid-Archean cratons are also characterized by lower crustal thicknesses (Archean median range = 32–39 km vs. post-Archean average = 41 km) and lower crustal seismic velocities. These observations are shown to be distinct from those observed in any modern-day tectonic environment. The data presented here are most consistent with a model in which Archean crust undergoes delamination of dense lithologies at the garnet-in isograd resulting in a flat, sharp Moho reflector and a thinner and more felsic-intermediate crust. We discuss the implications of this model for several outstanding paradoxes of Archean geology.

Contents

* Corresponding author.
E-mail address: dallashabbott@gmail.com (D.H. Abbott).

0040-1951/$ – see front matter © 2013 Elsevier B.V. All rights reserved.
http://dx.doi.org/10.1016/j.tecto.2013.09.014

1. Introduction

There is continuing controversy about the tectonic processes that produced Archean continental crust (Helmstaedt, 2009; Herzberg and Rudnick, 2013; Miller and Eaton, 2010; Rollinson, 2010; Wyman and Kerrich, 2009). Based on geochemical indices, modern continental crust seems to be largely of arc affinity (Taylor and McLennan, 1985, 1995), or at least extensively contaminated by arc-like processes (Condie, 1999, 2005; Jagoutz and Schmidt, 2012; Rudnick and Gao, 2003). However, the crust is differentiated, with a large component of silicic material that could not have originated from a single stage of mantle melting either in an arc or in a mantle plume. In contrast, the low Fe olivine (Mg# 93) [Mg# = Mg^{2+} / (Mg^{2+} + Fe^{Total}) × 100] in the Archean-age mantle roots of continental cratons seems to represent the residue from high degrees of partial melting—a possible Archean analog for mantle plume processes (Afonso et al., 2008). In this paper, we focus on tabulations of the characteristics of the lower crust and Moho within undisturbed Archean cratons and use this data set to constrain their genesis.

We consider the physical properties of the lower crust and the Moho. Our goal is to see how the properties of the lower crust and the sharpness of the Moho transition varies as a function of geological age and tectonic history, and how this may relate to the origin of the crust and underlying lithospheric mantle. In particular, we ask if the physical characteristics of the Moho relate in some fundamental way to the changes in lithospheric evolution since Archean time. This study has been preceded by numerous related studies that address more broadly the composition and physical properties of the lower crust (Christensen and Mooney, 1995; Fountain and Christensen, 1989; Griffin and O'Reilly, 1987; Holbrook et al., 1992; Mooney and Meissner, 1992; Rudnick and Fountain, 1995; Rudnick and Gao, 2003; Wedepohl, 1995).

2. Petrological and geophysical data sources

Moho depth has been determined on a global scale (Mooney et al., 1998). We define a sharp Moho as one where the crust/mantle transition occurs over a vertical distance of less than 2 km, e.g. (James et al., 2003). In areas with a more diffuse Moho, the crust/mantle transition commonly occurs over a minimum distance of 3 to 5 km. Previous studies of the Moho have primarily focused on its characteristics within different tectonic provinces (Cook, 2002; Cook et al., 2010; Hale and Thompson, 1982; Jarchow and Thompson, 1989; Mooney and Meissner, 1992). The study of Jarchow and Thompson (1989) provides a valuable historical perspective on the seismic Moho, and Cook et al. (2010) provides a detailed review of seismic reflection observations in different geological and age settings within Canada.

While there has been much discussion of the petrology of the Archean crust and sub-crustal lithosphere, the physical properties of the crust–mantle boundary (the Moho) also provide constraints on the processes by which the crust and lithospheric mantle were formed. The modern-day seismic Moho is defined as the depth at which the P-wave seismic velocity reaches values ≥7.6 km/s (Jarchow and Thompson, 1989; Steinhart, 1967). This depth typically coincides with the seismic reflection Moho, which is the boundary between the reflector rich crust and the reflector poor uppermost mantle (Cook, 2002; Cook et al., 2010; Mooney and Brocher, 1987). In addition to seismic refraction/wide-angle reflection profiles and vertical-incidence seismic reflection profiles, Archean crust has recently been investigated by studies that employ seismic receiver functions. The latter have provided a new look at the crust. Significantly, these studies rarely find strong seismic discontinuities within Archean crust; the most prominent discontinuity is generally the Moho itself (Kumar et al., 2012; Nguuri et al., 2001). In refraction studies, Archean crust can be divided into layers, but the Moho is usually the strongest discontinuity, a finding that is consistent with receiver function studies. Thus, a consistent feature of seismic studies of Archean crust is a sharp Moho boundary.

2.1. Moho and crustal characteristics: Part 1—Western Australia

In western Australia, there are two Archean cratons, the Pilbara block (3.7–2.9 Ga) and the Yilgarn block (3.0–2.7 Ga)(Griffin et al., 2004; van Kranendonk et al., 2007). They are separated by the 1.84 Ga Capricorn orogen. The Moho beneath both cratons is sharp and thin with one exception near the southern edge of the Pilbara block (Fig. 1, Tables 1,2) (Reading et al., 2012). The Moho is visible as a pronounced increase in seismic velocity over a depth range of 2 km or less. In contrast, the Moho beneath the younger Capricorn Orogen is diffuse. Indeed, of the three seismic stations within the Capricorn Orogen (WS06, WS05, and WS04), the Moho is detectable only at WS05. The crustal cross section (Fig. 1) shows two salient features (1) thinner crust (30–34 km) in areas of older Archean crust (3.65–3.15 Ga) and (2) a sharp Moho boundary for Archean crust as compared with the Proterozoic Capricorn Orogen.

2.2. Moho and crustal characteristics: Part 2—Canadian Shield

As in Australia, we also see age related trends in the character of the Archean crust of the Canadian Shield. From west to east, the cratonic crust of the Superior Province becomes progressively younger, from ca. 3.5 Ga in the Winnipeg River subprovince, to ca. 2.8–2.9 Ga in the eastern Wabigoon subprovince (Fig. 2). Seismic refraction and wide-angle reflection results from the Superior Province of the Canadian shield (Fig. 2) show the thinnest crust (~32–36 km) in the 3.5 Ga Winnipeg River subprovince (Davis et al., 2005; Musacchio et al., 2004) whereas the 2.8 Ga Wabigoon has a crustal thickness between 38 and 42 km. While the translation of seismic P-wave velocity into crustal composition can be misleading (i.e. Behn and Kelemen, 2003), lower P-wave velocities generally correspond to more evolved, Si-rich crustal compositions and higher P-wave velocities are associated with more mafic compositions. Average lower crustal velocities in the 3.5 Ga Winnipeg River subprovince are approximately 6.7 to 6.8 km/s. The 3.2–3.0 Ga Central Wabigoon subprovince has average crustal velocities of 6.8 km/s (in the west) up to 6.9 km/s in the east, and the 2.8–2.9 Ga Eastern Wabigoon subprovince has a lower crustal seismic velocity of 7.1 km/s. The high velocity in the Eastern Wabigoon subprovince most likely represents mafic underplating from the 1.1 Ga Keweenawan rifting event (Boerboom, 1994; Hansen, 1975). In summary, the seismic cross section from the Canadian Shield illustrates the general trend of thinner crust in older undisturbed Archean cratons and a possibly intermediate composition lower crust in pre 3.0 Ga cratons, compared with their post-Archean counterparts. The cross section does not provide much information on the sharpness of the Moho transition.

2.3. Moho and crustal characteristics: Part 3—Southern Africa

The contrast in Moho character between Archean cratons and post-Archean crust is best seen from the Kaapvaal and Zimbabwe cratons in

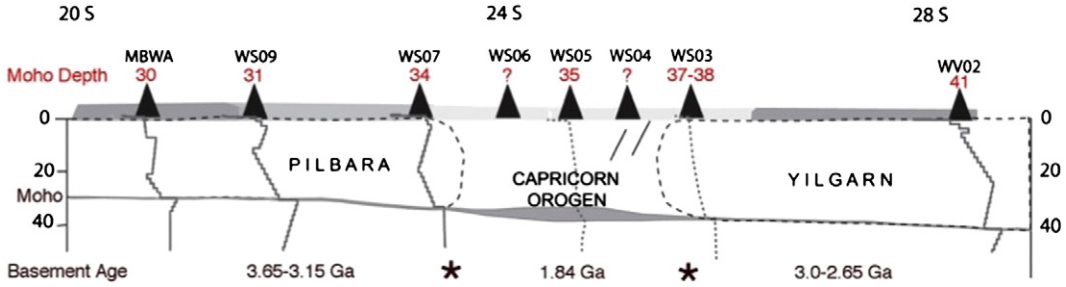

Fig. 1. After (Reading and Kennett, 2003). Representative cross section of crust and upper mantle from the north to south across the 3.65–3.15 Ga Pilbara block, the 1.84 Ga Capricorn orogen and the 3.0–2.65 Ga Yilgarn block in western Australia. Black solid cones: seismic stations. Dashed lines beneath stations extending to depth beneath WS07 and W02: extent of Archean crust. Red numbers: depth to Moho in km. Stars: boundaries between age provinces. Gray lines under solid cones: Seismic S-wave velocity versus depth. Gray subhorizontal line of varying thickness represents the location and thickness of the Moho.

southern Africa. Both the Kaapvaal and Zimbabwe cratons in southern Africa contain crustal fragments that formed as far back as 3.7 Ga (Compston and Kröner, 1988; Horstwood et al., 1999; Schoene et al., 2009). The Kaapvaal craton contains one of the oldest supracrustal sequences known, the Pongola basin. The sediments of the Pongola basin supergroup date back to 3.0 Ga (Hegner et al., 1994), implying that this part of the Kaapvaal craton was a stable continental block by 3.0 Ga. Additionally, the ages of the oldest sulfide inclusions in diamonds from beneath the Kaapvaal craton are within 100 million years of the overlying crust, suggesting that the lithospheric mantle below the craton was also stable (Pearson et al., 1995). The eastern part of the Zimbabwe craton (the Tokwe segment) was also stable very early, at 2.9 Ga. The Kaapvaal and Zimbabwe cratons were welded together at ca. 2.6–2.7 Ga, forming the Limpopo mobile belt and incorporating the ancient Limpopo microcontinent (De Wit et al., 1992). The final amalgamation of terranes to the Kaapvaal craton occurred at 2.5 Ga. Thus, although the Kaapvaal has a stabilization age of 3.0 Ga and the eastern Zimbabwe (Tokwe segment) has a stabilization age of 2.9 Ga, the composite craton, the Kalahari craton, has a stabilization age of 2.5 Ga.

De Wit and Tinker (2004) present eight deep seismic reflection profiles with a total length of 500 km from the central Kaapvaal craton. These data clearly depict a locally flat, sharp Moho, in agreement with previously reported seismic-refraction data that indicate a Moho transition that is 1–3 km thick (Durrheim and Green, 1992). Receiver function data from southern Africa also show a sharp, flat Moho over undisturbed parts of the Archean Kaapvaal and Zimbabwe cratons (James et al., 2003; Nguuri et al., 2001) (Fig. 3). The northern and southern marginal zones of the Limpopo belt also exhibit a sharp Moho transition. These zones have been interpreted as cratonic lithosphere overthrust by Proterozoic crust (De Wit et al., 1992). In contrast, the disturbed zones near the Bushveld complex, in the Limpopo belt and in off-craton mobile belts mainly exhibit a diffuse Moho (Fig. 3). The cratonic crust is generally thinner in the areas with a sharp Moho except for the marginal zones of the Limpopo belt where overthrusting caused crustal thickening. In addition to the sharp Moho, the crust–mantle boundary is also flat over a large geographical area within the Kaapvaal and Zimbabwe cratons, as compared with the more undulose crust–mantle boundary in neighboring non-cratonic areas.

Consistent with observations from western Australia and the Canadian Shield, the lower crust in the Kaapvaal craton (outside of the areas associated with the Bushveld Complex) and the Zimbabwe craton (outside of the Magondi mobile belt) also lacks the high velocity lower crust (Vp > 7.1 km/s) that is frequently found in nearby post-Archean crust (Kgaswane et al., 2009; Nguuri et al., 2001). Crustal xenolith and seismic studies have found that the lower crust in post-Archean areas is generally mafic (Christensen and Mooney, 1995; Rudnick and Fountain, 1995; Wedepohl, 1995). In contrast, xenolith and seismic data indicate that undisturbed lower crust in the Kaapvaal and Zimbabwe cratons (Kalahari craton) is intermediate or even felsic in composition (James et al., 2003; Niu and James, 2002; Schmitz and Bowring, 2003).

2.4. Evaluating the Moho transition from receiver function data

We have collected receiver function data on the Moho transition from as many cratonic areas as are recorded in the literature. In studies including a quantitative analysis of errors (Darbyshire et al., 2007; Nair et al., 2006; Thompson et al., 2010), an error in the Moho depth of less than ±0.8 km defines a sharp Moho. To obtain data from a sufficient number of locations, many of the studies we have included in our analysis provided no quantitative estimate of the sharpness of the Moho transition. In those cases, we have made a qualitative evaluation of the sharpness of the Moho. Representative examples are in Fig. 3. A sharp Moho has a bell shaped curve and an amplitude (where available) within ~60% of the maximum amplitude. The curve extends over a lateral distance of less than 12–14 km. The apparent depth extent of the curve does not reflect the actual thickness of the Moho transition. For example, Station sa19 has a Moho transition independently evaluated as less than 2.0 km thick (James et al., 2003). On Fig. 3, the receiver function peak at the Moho at station sa19 is about 12 km wide and has an amplitude in the middle part of the estimated range for a sharp Moho. A transitional sharp Moho has a slightly skewed bell shaped curve and an amplitude (where available) within ~50% of the maximum

Table 1
Receiver function results—Group 1: Stabilized 2.9–3.0 Ga.

Craton/age range, Ga	Sharp Moho, #	Diffuse Moho, #	Depth, km	References
Kaapvaal-outside Bushveld/3.7–3.0	35	0	33–45	Nguuri et al. (2001)
Kaapvaal near Kimberley/3.7–3.0	31	0	35.4 ± 0.2	James et al. (2003), Niu and James (2002)
Kaapvaal outside Bushveld/3.7–3.0	21	0	34–42	Nair et al. (2006)
Zimbabwe-east/3.8–2.9	7	0	34–37	Nguuri et al. (2001)
Zimbabwe-east/3.8–2.9	5	0	36.5–39	Nair et al. (2006)
Pilbara/3.7–2.9	3	0	30–34	Reading and Kennett (2003)
Pilbara/3.7–2.9	8	1	29–36	Reading et al. (2012)

Table 2
Receiver function results—Group 2: Stabilized 2.7–2.8 Ga.

Craton/age range, Ga	Sharp Moho, #	Diffuse Moho, #	Depth, km	References
Yilgarn/4.4–2.7	3	0	29–36	Reading et al. (2012)
Yilgarn/4.4–2.7	2	0	37–41	Reading and Kennett (2003)
Greenland/3.9–2.7	1	1	35–41	Kumar et al. (2007)
Rae/3.9–2.7	10	6	35–44	Thompson et al. (2010)
Superior/3.8–2.7	17	1	34–44	Darbyshire et al. (2007)
Hearne/3.0–2.7	0	5	37–41	Thompson et al. (2010)
Tanzanian/4.0–2.7	7	1	37–42	Last et al. (1997)

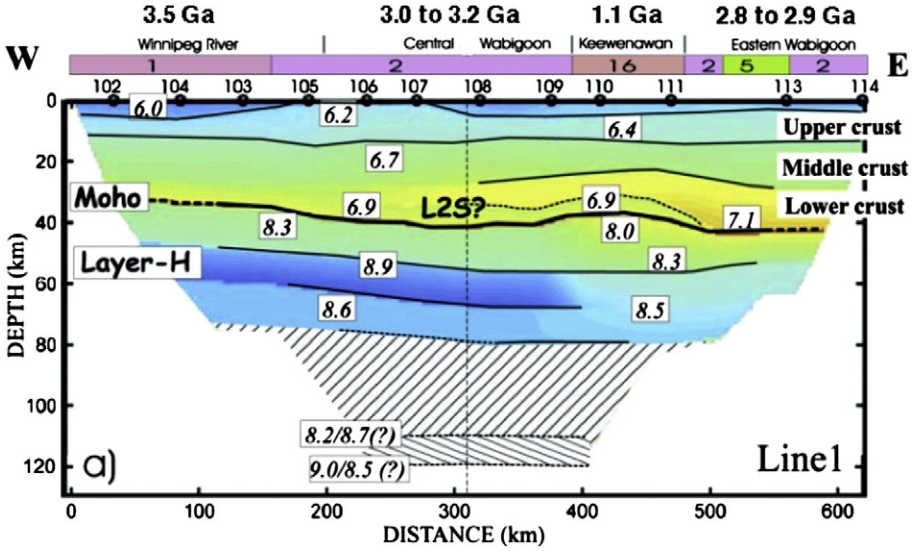

Fig. 2. After (Musacchio et al., 2004). Seismic line from the Winnipeg River subprovince to the Eastern Wabigoon subprovince of the Superior Province. Seismic velocities are constrained by seismic refraction point gathers (numbered dots on top of black box). Seismic velocities are labeled and color-coded. L2S is layer 2S, an anomalous lower crustal layer with a seismic velocity of 7.41 km/s. The colored line with numbers at the top of the plot just below the province names represents regional lithology: 1: felsic plutonic rocks, 2: intermediate plutonic rocks, 5: mafic to intermediate volcanic rocks, 16: mafic plutonic rocks.

amplitude. The curve extends over a lateral distance of less than 15 km. A transitional diffuse Moho has an irregular shaped pulse, 15–20 km wide with a maximum amplitude less than ~40% of the maximum amplitude in the study. A diffuse Moho has an irregular pulse over 15 km wide with a maximum amplitude less than ~30% of the maximum amplitude in the study.

When we quantitatively compare the Moho transition between off-craton and on-craton sites in the Kaapvaal–Zimbabwe craton (Fig. 3), there are clear differences. The mean on-craton score is 1.23 ± 0.16 (95% confidence) and the mean off-craton score is 2.79 ± 0.35 (95% confidence). A Z-test indicates that the null hypothesis that the two means differ only because of random variation can be rejected to better than 99% probability. When applied to the observed histograms, a Pierson's chi-squared test indicates that the null hypothesis that that the two histograms are drawn from the same underlying distribution can be rejected to greater than 99% confidence. Hence we conclude that the on- and off-craton scores are statistically distinguishable.

The differences in sharpness of the Moho have tectonic significance. For example, one of the two "on-craton" sites (sa71) with an apparent diffuse Moho was classified as part of the off-craton Limpopo belt by later workers (Gore et al., 2009). The second "on-craton" site with a diffuse Moho (sa43) is very close to the surface outcrop of the Bushveld complex. More recent receiver function studies show that the intrusion of the Bushveld complex affected a much broader region of the Kaapvaal craton than had previously been recognized (Youssof et al., 2013–in this volume). Their work shows that the amplitude of the Moho conversion, a rough proxy for the sharpness of the Moho, is greatest in areas of undisturbed Archean crust stabilized by 2.9–3.0 Ga.

2.5. Seismic observations: other Archean cratons

We have tabulated seismic observations from other Archean cratons (Tables 1–5). As emphasized by Cook et al. (2010), there is considerable variability in the character of the Moho (as imaged with seismic methods) from region to region. Different seismic methods are better at seeing different aspects of the crust and Moho. Several workers have described the resolution of the seismic velocity contrast and thickness of the Moho from seismic refraction and reflection data (Braile and Smith, 1975; Cook, 2002; Cook et al., 2010; Hale and Thompson, 1982; Jarchow and Thompson, 1989; Mooney and Brocher, 1987).

Receiver function studies that look at P to S conversions at the Moho are quite effective at imaging the sharpness of the Moho discontinuity. Receiver functions also detect the existence or absence of large-scale crustal convertors (i.e., seismic boundaries with a significant velocity contrast). We use a compilation of seismic properties derived using the receiver function method to produce a quantitative estimate of the relative proportions of sharp and diffuse Mohos within Archean cratons with differing ages of stabilization (Fig. 4).

3. Definition of stabilization age of cratonic blocks

Although many cratons contain areas of early Archean crust (pre-3.6 Ga), their Moho and crust were subsequently modified by deformation and plutonism over hundreds of million years until the craton became tectonically stable. At that time, most or all plutonic activity ceased and the surface of the craton was covered by sediment. Individual sedimentary layers became laterally extensive and contained sediment types typical of stable continental platforms: clean carbonate, shale and sandstone (Eriksson and Donaldson, 1986; Eriksson and Fedo, 1994; Lowe, 1980). In many cases, the sediments were intermittently covered with flood basalts (Blake, 1993; Eriksson et al., 2002), just as flood basalts cover some continental platforms today (e.g. the Permo-Triassic Siberian traps and the Triassic–Jurassic CAMP basalts.) Thus stable cratons are typically covered by continental platform sediments and/or flood basalts.

In our compilation, we divide Archean cratons into three age groups based on the age at which a craton became tectonically stable. The age of stabilization is the basal age of the oldest stable platform sediments: e.g. quartz arenite, clean carbonate and shale that are deposited upon the cratonic basement. The argument is that these sediment types imply no ongoing or recent tectonic activity. Because tectonic activity can come and go over geological time, the stabilization age is the age of earliest stability of the cratonic block.

The stabilization age should not be confused with the ages of the oldest rocks and minerals on each craton, which are generally far older (Table 5). With a few notable exceptions (Abitibi and Hearne in the Canadian shield), each craton contains some rocks older than 3.0 Ga. Almost all Archean cratons experienced significant igneous magmatism for periods longer than all of Phanerozoic time (Significant igneous magmatism includes basaltic through granitic intrusions but

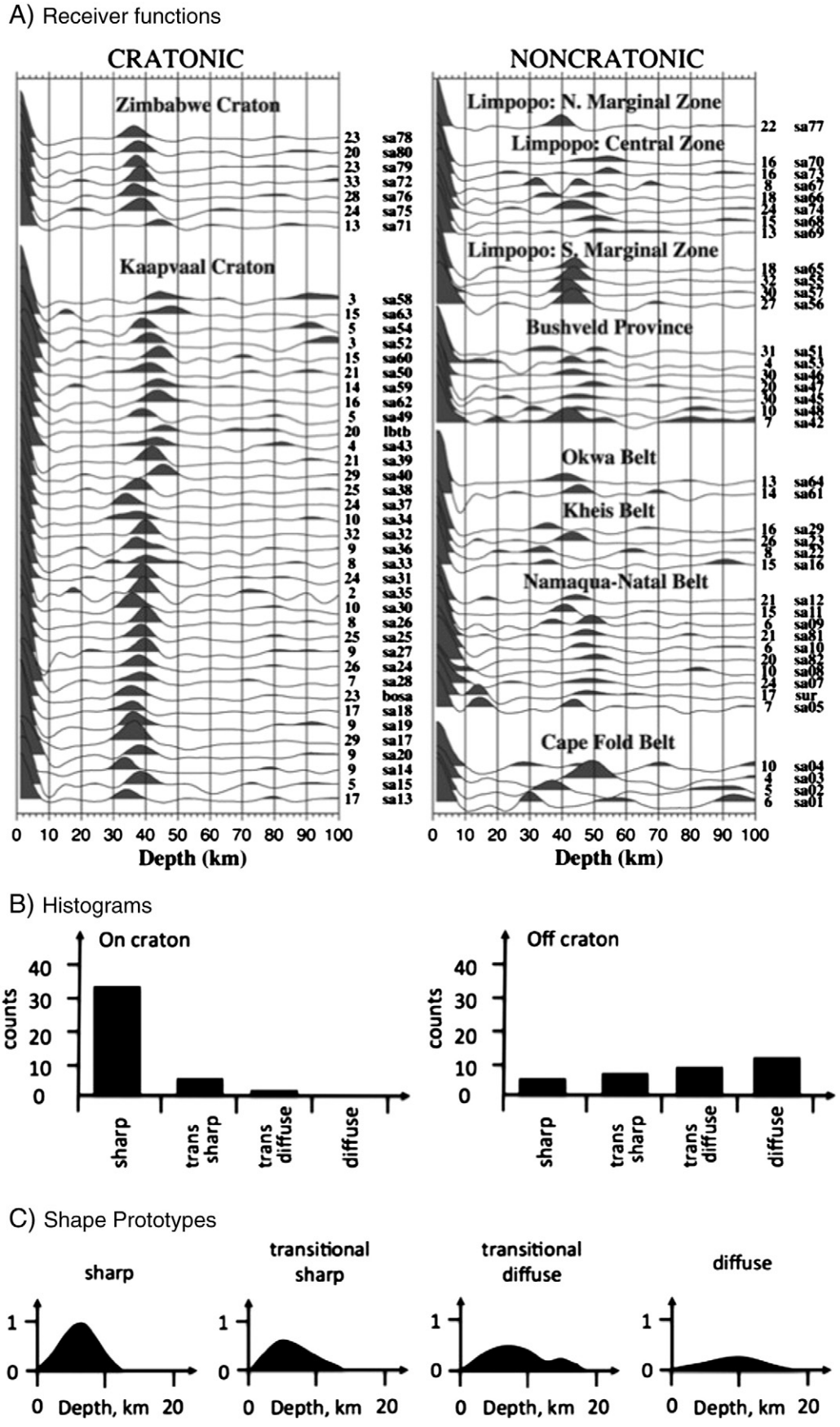
A) Receiver functions
CRATONIC
NONCRATONIC
Zimbabwe Craton
Kaapvaal Craton
Limpopo: N. Marginal Zone
Limpopo: Central Zone
Limpopo: S. Marginal Zone
Bushveld Province
Okwa Belt
Kheis Belt
Namaqua-Natal Belt
Cape Fold Belt
Depth (km)
B) Histograms
On craton
Off craton
counts
sharp
trans sharp
trans diffuse
diffuse
C) Shape Prototypes
sharp
transitional sharp
transitional diffuse
diffuse
Depth, km

Table 3
Receiver function results—Group 3: Stabilized 2.6–2.5 Ga.

Craton/age range, Ga	Sharp Moho, #	Diffuse Moho, #	Depth, km	References
Slave/4.0–2.6	10	2	36–40	Bank et al. (2000)
Baltic/3.7–2.6	8	6	45–50	Alinaghi et al. (2003)
Baltic/3.7–2.6	0	10	48–55	Kozlovskaya et al. (2008)
Sao Francisco/3.8–2.6	1	3	38–43	Assumpção et al. (2002)
N. China/4.0–2.5	8	0	32–48	Chen et al. (2010)
N. China/4.0–2.5	21	8	29–37	Zheng et al. (2007)
Yangtze/3.8–2.5	9	0	32–48	Chen et al. (2010)
Aravalli-Bundelkhand/ 3.3–2.5	3	0	36–38	Kumar et al. (2012)

excludes low degree partial melts like kimberlites, lamproites and alnoites.).

The stabilization age may be nearly the same as the age of plate tectonic amalgamation of a craton but it may also be significantly different. For example, the plate tectonic amalgamation of the entire Canadian shield was at ~1.8 Ga (Hoffman, 1988). In contrast, portions of the Canadian shield contain 3.0 Ga stable platform sediments (Eriksson and Donaldson, 1986; Sasseville et al., 2006). We endeavored to estimate stabilization age in a consistent manner, but we recognize that future, more detailed studies will find more complexity and will subdivide cratonic blocks.

4. Receiver function results and stabilization age

The first group of cratons stabilized between 2.9 and 3.0 Ga (Tables 1,4,5). These three cratons, the eastern Zimbabwe craton, the Kaapvaal craton, and the Pilbara block show sharp Mohos with one notable exception on the southern edge of the Pilbara block. Crustal thicknesses of these blocks range from 29 to 45 km. The second group of cratons became tectonically stable between 2.7 and 2.8 Ga (Table 2). These cratonic blocks have a high percentage of sharp Mohos (74%) but a notable percentage of diffuse Mohos (error in Moho depth of less than ±0.8 km). The youngest group became stable between 2.5 and 2.6 Ga (Table 3) and has the lowest percentage of sharp Mohos (67%). We see a progression: the percentage of sharp Moho discontinuities declines as the age of stabilization of the craton becomes younger (Fig. 5). There is a clear difference between the percentage of sharp Moho for cratons stabilized at 2.9–3.0 Ga and slightly younger terranes (2.7–2.8 Ga). It is not clear that there is a statistically significant difference between the two youngest groups (2.7–2.8 Ga) and (2.5–2.6 Ga).

Table 4
Receiver function results on Moho sharpness and depth.

Stabilization age	Sharp Moho, #	Diffuse Moho, #	Sharp, %	Moho depth, km	Median depth, km
2.9–3.0 Ga	110	1	99	29–45	32–39
2.7–2.8 Ga	40	14	74	29–44	33–40
2.5–2.6 Ga	60	29	67	29–55	33–52
All Archean	210	44	83	29–55	32–52
2.5–2.8 Ga	100	43	70		

Table 5
Oldest age and stabilization age references for cratonic blocks.
*** model age Nd, Hf **d detrital zircon age ** inherited zircon age, *primary igneous zircon.

Craton	OA, Ga	Oldest age OA Ref.	SA, Ga	Stabilization age SA Ref.
Kaapvaal	3.7*** 3.7*	Schoene et al. (2009)	3.0	Armstrong et al. (1991), Moser et al. (2001), Zeh et al. (2009)
E. Zimbabwe Tokwe, Sebwakian	3.8** 3.6*	Dodson et al. (1988), Nägler et al. (1997), Horstwood et al. (1999)	2.9	Moorbath et al. (1987), Dodson et al. (2001), Fedo et al. (2003)
Pilbara Block	3.7** 3.5*	Thorpe et al. (1992)	2.9	Blake (1984), Van Kranendonk et al. (2007)
Yilgarn	4.4** 3.7*	Thern and Nelson (2012)	2.7	Czarnota et al. (2010), Ivanic et al. (2012)
Greenland	3.9*	Nutman et al. (2007), Nutman et al. (2009)	2.7	Eriksson and Fedo (1994), Nutman and Friend (2007), Friend et al. (2009)
Rae	3.9*** 3.6**	Hartlaub et al. (2005)	2.7	Hartlaub et al. (2004), Sandeman et al. (2005)
Superior*	3.8*	O'Neil et al. (2007)	2.7	Card (1990), Corfu and Stott (1993), Davis et al. (2005)
Hearne	3**	van Breemen et al. (2007)	2.7	Hoffman (1988), Sandeman et al. (2004)
Tanzanian*	4** 3.6*	Kabete et al. (2012)	2.7	Bellucci et al. (2011), Lawley et al. (2013)
Slave*	4.1*** 3.8**	Bowring et al. (1989), Stern and Bleeker (1988), Bowring and Williams (1999)	2.6	Helmstaedt (2009), Corcoran (2012)
Baltic*	4.0*** 3.7** 3.5*	Slabunov et al., 2006; Lauri et al., 2011	2.6	Gorbatschev and Bogdanova (1993), Mänttäri and Hölttä (2002), Mikkola et al. (2011)
Sao Francisco	3.8**d 3.1*	Hartmann et al. (2006), Rios et al. (2008)	2.6	Peucat et al. (2011)
N. China	3.8* 4***	Liu et al. (1992), Song et al. (1996), Zheng et al. (2004), Geng et al. (2012)	2.5	Zhao et al. (2005), Han et al. (2012), Ma et al. (2012)
Yangtze	3.0* 3.8**d	Zhang et al. (2006)	2.5	Zheng et al. (2006)
Aravalli-Bundelkhand	3.3** 3.3**d 3.7***	Kaur et al. (2011)	2.5	Roy and Kröner (1996), Wiedenbeck et al. (1996), Roy et al. (2005), Meert et al. (2010)
Nain-Hopedale	3.1* 3.3***	James et al. (2002)	2.8	James et al. (2002)
Abitibi	2.7* 2.8**	Davis (2002)	2.7	Chown et al. (2002)
Winnipeg River	3.2* 3.5***	Davis et al. (2005)	2.7	Corfu (1996)
Wabigoon	3.1* 3.3**d 3.4***	Davis et al. (2005), Henry et al. (2000)	2.7	Tomlinson et al. (2004)
Uchi	2.9* 3.2***	Henry et al. (2000)	2.7	Corfu and Stott (1993)
Behrens R./N. Caribou	3.0* 3.2***	Henry et al. (2000)	2.7	Corfu and Stott (1993)
Nain-Saglek	3.8* 3.9**	Schiøtte et al. (1989), Schiøtte et al. (1993)	2.6	Connelly and Ryan (1996)
Dharwar	3.3* 3.6**d	Nutman et al. (1992), Naha et al. (1993)	2.5	Balakrishnan et al. (1999)

5. Thickness range of the crust

We find that the range in crustal thickness shows a distinct trend with stabilization age of the craton (Table 4, Fig. 6). The cratons with the oldest stabilization ages of 3.0–2.9 Ga have crustal thickness ranges of 29–45 km and a median crustal thickness of 32–39 km. (Each study produces a crustal thickness range and the median value of the crustal thickness range of each craton is the median crustal thickness.) The Archean cratons with intermediate stabilization ages of 2.8–2.7 Ga have crustal thickness ranges of 29–44 km and a median crustal

Fig. 3. (A) Sharp Moho (Archean craton) versus diffuse Moho (non-cratonic) as imaged by teleseismic data from southern Africa. Clear, well-aligned phases that are converted waves from a sharp Moho boundary are evident as strong pulses on undisturbed cratonic crust. Non-cratonic crust and disturbed cratonic crust lack such clear, well-aligned seismic pulses due to an uneven, diffuse Moho boundary (James et al., 2003). Numbers to the right of each receiver function profile are the number of earthquakes used to calculate the receiver function (near right) and the abbreviation for the seismic station (far right). (B) Histograms of the distribution of sharp (1), transitional sharp (2), transitional diffuse (3), and diffuse (4) between cratonic and off craton crust. (C) Prototypes of the shapes of Moho transitions: sharp (1) transitional sharp (2), transitional diffuse (3) and diffuse (4).

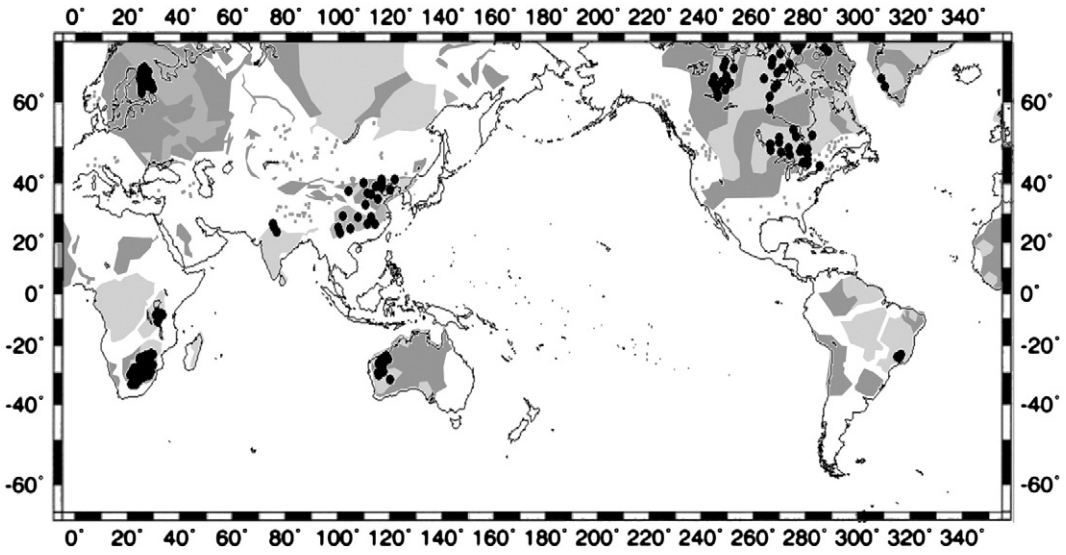

Fig. 4. Map of Archean cratons (light gray) and Early Proterozoic cratons (dark gray). Black circles: locations of seismic stations with receiver function results. Original map from (Abbott et al., 2000). Map has been updated with more current information on basement age.

thickness of 33–40 km. The Archean cratons with the youngest stabilization ages of 2.6–2.5 Ga exhibit a crustal thickness range of 29 to 55 km and a median crustal thickness range of 32–52 km. While the differences in median crustal thickness between these three groups are small, the global trend to greater crustal thickness with younger stabilization age is consistent with the trend observed for individual cratons (as shown above) and with the higher average crustal thickness observed in the modern-day continental crust (ca. 41.1 km; Christensen and Mooney, 1995). Unlike the Moho sharpness, the crustal thickness data derived from receiver functions (Table 4, Fig. 6) shows the biggest differences between crust with stabilization ages of 2.8–2.7 Ga and crust with stabilization ages of 2.6–2.5 Ga.

6. Sharp and diffuse Mohos and the nature of Archean crust

Receiver function data show that areas of undisturbed Archean crust with sharp Moho boundaries have few internal seismic convertors (Fig. 3). In most cases, the Moho is the strongest seismic convertor in the crustal section. In contrast, areas of disturbed Archean crust like the Bushveld Complex have one or more strong seismic convertors within the crust (James et al., 2003; Nguuri et al., 2001). Because internal seismic convertors scatter seismic energy, they diminish the amplitude of the Moho phase, making the Moho more difficult to identify. They can also make the Moho phase appear more diffuse. When data processing is improved (Nair et al., 2006), resolution of the Moho improves in receiver functions.

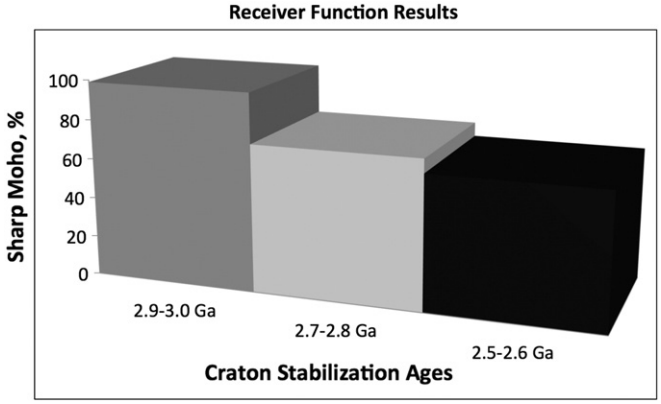

Fig. 5. Stabilization age of cratons (Ga) versus sharpness of the Moho (%). Receiver function results.

7. Flatness of the Archean Moho

The general sharpness of the Archean Moho is accompanied by smoothly varying, relatively small lateral changes in crustal thickness. This can be seen in all of the seismic data sets (Figs. 1–3). In contrast, the Moho in post-Archean mobile belts in southern Africa (Fig. 3) shows abrupt ups and downs that appear random, at least on the scale of the distance between seismic stations.

8. Discussion of receiver function results

The trends in Moho sharpness, Moho smoothness and crustal homogeneity are consistent with temporal variations in crustal evolution. Early to late Proterozoic orogens surrounding Archean cratons most

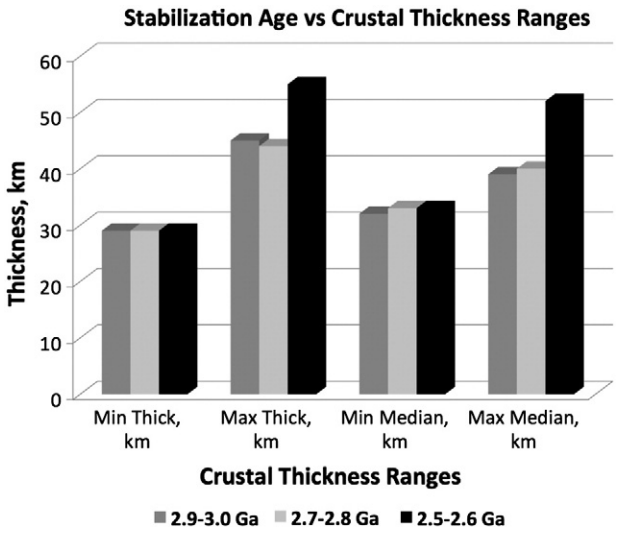

Fig. 6. Stabilization age of cratons (Ga) versus crustal thickness ranges for all cratons in an age group; minimum thickness, maximum thickness, minimum value of median thickness, and maximum value of median thickness.

often have a diffuse Moho (Figs. 1 and 3). Crustal thicknesses of Proterozoic orogens surrounding late Archean cratons are sometimes similar to those of the associated Archean crust (Tugame et al., 2012). The biggest change in Archean crustal thicknesses appears between ~2.7 and 2.6 Ga (Table 4, Fig. 6) as opposed to the biggest change in sharpness of the Archean Moho between ~2.9 and 2.8 Ga. A slowly varying depth to the Moho and an absence of internal crustal seismic convertors seem to be coupled in many areas of Archean crust but are not found everywhere. In contrast, areas of post Archean crust tend to exhibit rapid variations in crustal thickness and one or more seismic convertors. All of these changes provide an indication that crustal formation and preservation evolved during Archean time. We discuss this more fully later.

8.1. Seismic reflection and refraction results from Archean cratons

Seismic reflection and refraction data are both excellent tools for resolving intracrustal reflectors. Because the seismic frequencies of the controlled sources used in seismic reflection studies are higher than those of the earthquakes employed in receiver function studies, seismic reflection data provide the highest resolution of seismic discontinuities within the crust. Seismic reflection data provide good two way travel time estimates for a given crustal reflector but cannot resolve the seismic velocity structure of the crust beyond the upper few km. Thus, seismic reflection data alone cannot reveal the exact thickness of the crust. Because internal reflectors can reduce the strength of the Moho return, seismic reflection lines may image the Moho as diffuse in areas where lower frequency receiver function data show a sharp Moho, e.g. (de Wit and Tinker, 2004).

In seismic refraction lines, the sharpness of the Moho is determined from the character of the Moho reflection (PmP). This reflection is clearly resolved in crust where the Moho transition is sharp, and is less well resolved in crust where the Moho transition is diffuse (Braile and Smith, 1975; Stein and Wysession, 2003). Where the Moho is sharp the seismic velocity versus depth function shows an abrupt increase at the Moho transition. Where the Moho is diffuse, the seismic velocity versus depth function shows a gradual increase at the Moho transition.

Seismic refraction/wide angle reflection profiling (here abbreviated as seismic refraction) is the best method of resolving the velocity structure of the crust (Mooney, 1989). A larger velocity contrast increases the amplitude of the return from a seismic reflector like the Moho, so seismic refraction profiles provide the opportunity to determine if the seismic velocity structure of typical Archean crust is different from that of post-Archean crust. Earlier studies (Durrheim and Mooney, 1994) argued that the lower crust within Archean cratons was silicic to intermediate in contrast to the basaltic lower crust in Proterozoic terranes. A basaltic lower crust has on average a high seismic velocity that creates a lower velocity contrast with the underlying mantle compared with a silicic or intermediate lower crust. Thus, we hypothesize that some of the difference between the typical Archean Moho and the post Archean Moho is due to differences in the lower crustal composition as evidenced by the seismic velocity of the lower crust.

8.2. Assessing crustal composition from seismic refraction data

Recent work has shown that at higher pressures typical of the lower crust, seismic P wave velocity can be translated into composition with a relatively high degree of confidence (Behn and Kelemen, 2003). If the seismic P-wave velocity is higher than 7.1 km/s, the lower crust is most likely basic (basaltic) in composition. If the seismic P-wave velocity is lower than 6.8 km/s, the lower crust is most likely silicic (granitic) in composition. In both cases, the lower crust will consist of high-grade metamorphic rocks. We use their results to estimate the composition of the lower crust within Archean cratons.

9. Seismic refraction and reflection results

Table 6 shows seismic reflection and refraction results sorted by age of crustal stabilization. The data set is not as complete as that from receiver functions but we see some general trends. Where the seismic refraction data constrain a narrow range in lower crustal velocities of 0.2 km/s or less, crust with stabilization ages of 3.0 to 2.6 Ga has a lower crust that is felsic or felsic to intermediate in composition (Fig. 7). It is only the Dharwar craton with a stabilization age of 2.5 Ga where the lower crust has an unequivocally basic composition. In refraction data where the lower crust has a broad range in velocities, the lower crust is characterized as intermediate to basic and there is no significant trend with stabilization age (Figs. 7 and 8, Table 6).

10. Refraction results on the sharpness of Moho

The one refraction study of cratonic crust stabilized by 2.9 Ga shows a uniformly sharp Moho (Table 7, Fig. 9). The refraction studies of crust stabilized between 2.8 and 2.7 Ga found that 88% of the crust had a sharp Moho. The refraction studies of crust stabilized between 2.6 and 2.5 Ga found that 60% of the crust had a sharp Moho. Even though the errors are large, the differences between the datasets appear to be significant. Overall, the more sparse refraction data is consistent with our receiver function trend in decreasing sharpness of the Moho with decreasing stabilization age of the cratonic block.

The refraction data show that those parts of Archean cratons with a basaltic lower crust have a sharp Moho in some places (e.g. the Dharwar) (Table 6). This is also apparent in seismic reflection profiles with velocities constrained by seismic refraction (Musacchio et al., 2004). This result implies that in areas where the lower crust is intermediate to silicic in composition the sharpness of the Archean Moho is not due solely to a large velocity contrast between the lower crust and the

Table 6
Seismic Results with Seismic Velocity/Crustal Composition. REFL—seismic reflection, RF—receiver function, REFR—seismic refraction. Comp LC—lower crustal composition. Intermed—intermediate andesitic crustal composition, basic—basaltic, felsic–dacitic composition.

Craton/Age, Ga	Data type	Moho type	Depth, km	Vp-LC, km/s	Comp LC # in Fig. 7	Reference
Kaapvaal/3.7–3.0	REFL	Sharp-to-diffuse	36–41	–		deWit and Tinker (2004)
Kaapvaal/3.7–3.0	RF	Sharp-31, Diffuse-0	35.4 ± 0.2	6.75	felsic #1	James et al. (2003), Niu and James (2002)
Pilbara/3.7–2.9	REFR	Sharp-8, Diffuse-0	25–35	6.8–7.2	Intermed to basic #2	Drummond (1988)
Nain-Hopedale/3.3–2.8	REFR	Diffuse-1	32	6.65–6.7	Felsic #3	Louden and Fan (1988)
Yilgarn/4.4–2.7	REFL	Diffuse	33–38	–		Drummond et al. (2000)
Yilgarn/4.4–2.7	REFR	Sharp-5, Diffuse-0	25–35	6.8–7.2	Intermed to basic #4	Drummond (1988)
Abitibi/2.8–2.7	REFL	Sharp	38–40	–		Calvert et al. (1995)
Abitibi/2.8–2.7	REFR	Sharp-10, Diffuse-1	37–40	6.9–7.3	Intermed to basic #5	Grandjean et al. (1995)
Superior/3.8–2.7	RF	Sharp-17, Diffuse-1	34–44	–	Intermed to basic	Darbyshire et al. (2007)
Winnipeg R./3.5–2.7	REFR		32–40	6.7–6.8	Felsic #6	Musacchio et al. (2004)
Baltic/3.7–2.6	REFL	Sharp-to-diffuse	37–45	–	–	Mints et al. (2009)
Slave/4.0–2.6	REFR	Sharp-4, Diffuse-0	33	6.6–6.9	Felsic to intermed #7	Fernández Viejo and Clowes (2003)
Nain-Saglek/3.9–2.6	REFR	Sharp-0; Diffuse-1	28–32	6.7–6.9	Felsic to intermed #8	Funck et al. (2008)
Dharwar/3.6–2.5	REFR	Sharp-5, Diffuse-5	42–45	7.3	Basic #9	Mall et al. (2012)

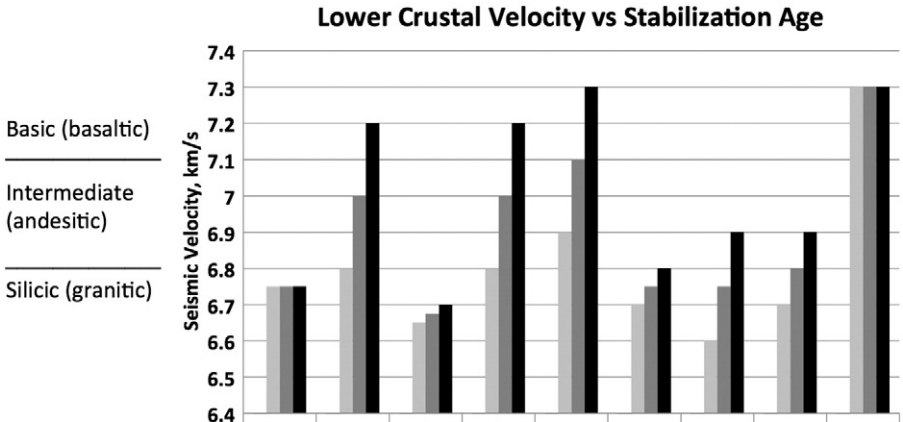

	1	2	3	4	5	6	7	8	9
Stabilizaton Age	3	2.9	2.8	2.7	2.7	2.7	2.6	2.6	2.5
Min Velocity	6.75	6.8	6.65	6.8	6.9	6.7	6.6	6.7	7.3
Average Velocity	6.75	7	6.675	7	7.1	6.75	6.75	6.8	7.3
Max Velocity	6.75	7.2	6.7	7.2	7.3	6.8	6.9	6.9	7.3

Fig. 7. Seismic velocity of the lower crust versus stabilization age. Data is from the 9 seismic refraction studies with lower crustal velocity results (Table 6). Groups 1–9 on the plot are delineated in parenthesis in the composition column of Table 6.

underlying mantle. Part of the sharpness is due to an abrupt change in bulk seismic velocity at the Moho as opposed to a slow change in bulk seismic velocity spread over a depth range of 2 km or more (James et al., 2003).

10.1. Comparison with modern-day crustal formation

The sharp Moho and flat crust–mantle boundary within most Archean cratons contrast strongly with the more diffuse and varying Moho that is frequently found in post-Archean terranes. Modern-day continental crust is thought to be produced in island-arc type settings, where the composition of the newly formed arc crust is similar to that observed globally for bulk continental crust (Jagoutz et al., 2011).

10.1.1. Island arcs

Seismic cross sections of modern arcs have several notable features (Fig. 10) and (Kodaira et al., 2010; Takahashi et al., 2008). The first is that the Moho is diffuse. As can be seen in Fig. 10, the Moho is imaged as a broad transition zone, occurring between regions characterized by Vp = 7.2–7.4 km/s and underlying regions with Vp = 7.6–7.8 km/s with no sharp change in seismic velocity as is typically observed in the cratons (Figs. 1,2). The second feature is the presence of higher seismic velocities within the lower crust compared with those observed in Archean cratons (Vp = 6.7–7.1 km/s, Table 6, Fig. 7). The third distinctive feature of modern arcs is the undulose nature of the Moho. The Moho depth can change by 10 km over a 50 km lateral distance. The undulose Moho is observed both in cross sections and along strike of arcs (Calvert et al., 2008; Kodaira et al., 2010; Takahashi et al., 2008).

The diffuse nature of the Moho, the higher seismic velocities in the lower crust and the undulose nature of the Moho boundary are significantly different from nearly all examples of Archean crust. The seismic velocities of the lower crust are all in the range of basaltic compositions rather than the range that is more typical of the intermediate compositions found within Archean lower crust.

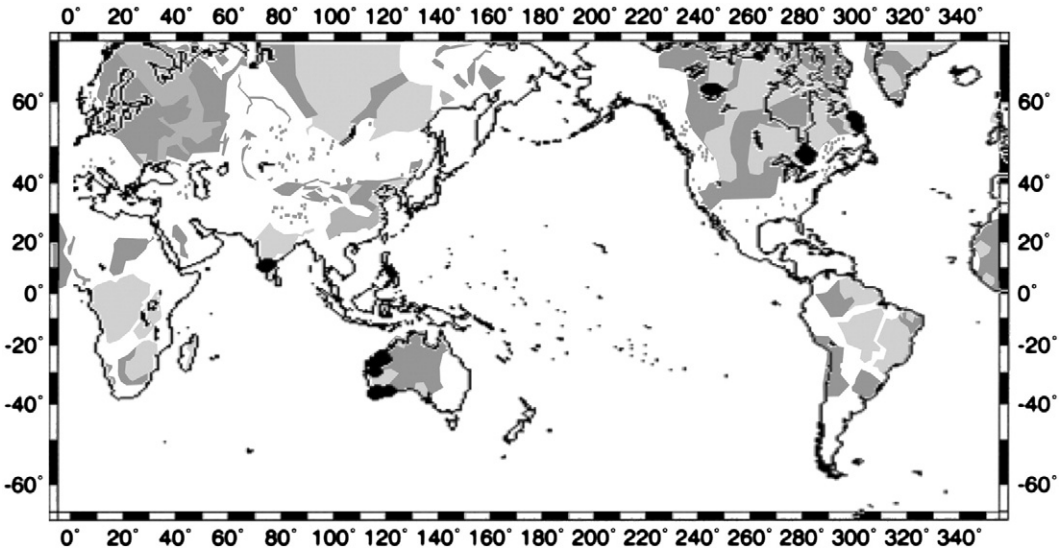

Fig. 8. Map of Archean (light gray) and Early Proterozoic blocks (dark gray). Black circles: locations of refraction lines used in estimating sharpness of the Moho. Original map from (Abbott et al., 2000). Map has been updated with more current information on basement age.

Table 7
Summary of refraction results on the sharpness of the Moho.

Stabilization age, Ga	Sharp, #	Diffuse, #	Sharp, %	1 Pt. Error, %
2.9–3.0	8	0	100	13
2.7–2.8	15	2	88	6
2.5–2.6	9	6	60	11
All Archean	32	8	80	2
All 2.5–2.8 Ga	24	8	75	3

10.1.2. Oceanic plateaus

The other commonly proposed modern analog for Archean protocontinents are oceanic plateaus, in particular Ontong Java. The crust of the thickest part of the Ontong Java Plateau reaches that of the thinner Archean continental crust (35 km) (Durrheim and Mooney, 1991; Furumoto et al., 1976; Miura et al., 2004). The seismic refraction study of Miura et al., 2004 shows clear PmP reflections over long distances for 6 out of 8 OBS record sections. The Moho in that part of the Ontong Java plateau is typically sharp. The Moho in some parts of the Ontong Java is relatively flat, but this is not true for the central Ontong Java.

The seismic velocities of the lower crust of the Ontong Java plateau range from 7.2 to 7.7 km/s, higher than those of Archean lower crust. In the central Ontong Java plateau, however, the lower crust has seismic velocities of about 7.1 km/s, within the range of some Archean lower crust (Table 6, Fig. 7). The crust–mantle boundary of the Ontong Java plateau has low relief in two cases (Fig. 11A, C) but shows rapid lateral changes in thickness in another case (Fig. 11B). The seismic structure of the Ontong Java plateau, and by inference other oceanic plateaus, is a better analog to Archean cratons than that of modern-day island arcs, however neither of these modern-day tectonic analogues satisfy all of the observations made for Archean cratonic crust.

11. Models for the production of a flat and sharp Moho within Archean cratons

The observations presented in this manuscript reveal that most Archean cratons are characterized by thinner than average crust with low-to-intermediate lower crustal seismic velocities (Vp = 6.7–7.1 km/s) and a flat, sharp seismic Moho. The flat, sharp Moho is inconsistent with the formation of the cratonic crust in an unmodified subduction zone-type setting, which typically results in the highly undulose and diffuse Moho reflectors observed at modern-day island arcs (Fig. 10). Furthermore, active upwelling (plume) dominated processes, such as those responsible for modern-day oceanic plateaus, can also be ruled out due to the highly basaltic nature of the plateau crust and higher seismic velocities of such occurrences (i.e. Ontong Java lower crustal Vp = 7.1–7.7 km/s) compared with the Archean cratons. The only persistent modern-day occurrence of sharp, flat Moho reflectors is within typical oceanic crust (Boudier and Nicolas, 1995; Collins et al., 1986; Vera et al., 1990), however the oceanic crust is also basaltic and therefore a poor analogue for the formation of the felsic-to-intermediate composition of Archean continental crust.

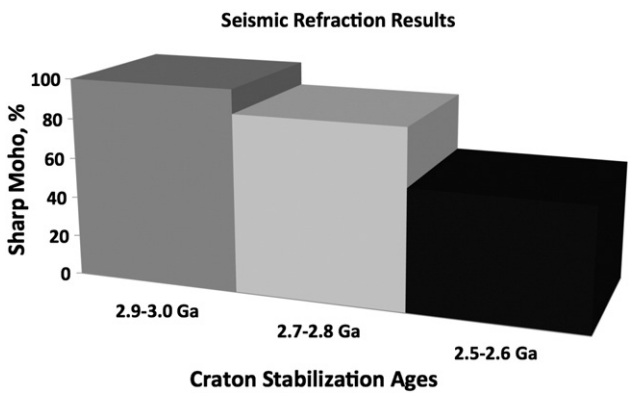

Fig. 9. Distribution of sharp Mohos from seismic refraction data.

One model for the stabilization of Archean cratons that does satisfy all of the four main constraints (sharp and flat Moho, and thinner-than-average crust with a felsic- to intermediate composition) is crustal delamination. Delamination will occur when portions of the lower crust become denser than the underlying mantle (Arndt and Goldstein, 1989; Kay and Mahlburg Kay, 1983). Due to the high density of garnet, which would be stable in primary Archean crust for depths greater than 25–30 km (Vantongeren and Korenaga, 2012), lower crustal rocks in the Archean were likely gravitationally unstable with respect to the underlying mantle. Delamination of garnet-bearing lithologies would therefore selectively remove the most mafic portions of the Archean crust, leaving behind a more felsic crust, explaining the thinner than average crust and the felsic-to-intermediate composition (and lower seismic velocities) observed for cratonic crust today.

The delamination hypothesis explains the preservation of a sharp, flat Moho despite the very long evolution of the cratons (hundreds of million years) from the time of the formation of the first granites and basalts until they became stable continental blocks (deWit et al., 1992; Smithies et al., 2009; Zhang et al., 2006). Upper crustal rocks in Archean cratons show clear evidence of deformation, however, the lithospheric roots of the cratons were preserved with apparently little deformation (Figs. 1–3).

In addition to satisfying the geophysical constraints presented here, the delamination hypothesis also explains some paradoxes of Archean tectonics. The first is the geochemical mass balance paradox that is based on the unique composition of Archean crust (Herzberg and Rudnick, 2013; Zegers and van Keken, 2001). This felsic to intermediate composition requires the loss of more than 80% of mafic Archean residues based on reasonable estimates of primary magma compositions e.g. (Herzberg et al., 2010). The second paradox is the rarity of Archean eclogites, which would be a common rock type if subduction were the dominant process. A study of kimberlites where eclogites were perceived as abundant (i.e. Roberts Victor, Bobbejean and Udachnaya) found that eclogites made up about 3–15% of the mantle xenolith suite (Schulze, 1989). The oldest known eclogitic inclusions in subcontinental lithospheric mantle are about 3.0 Ga (Helmstaedt, 2010; Shirey and Richardson, 2011), but these are exceedingly rare. If basaltic protocrust was destroyed relatively rapidly by a combination of partial melting and density driven removal, the basalt would not be preserved as eclogite within the lithospheric mantle. The third paradox is the absence in most Archean cratons of linear belts of granitic to basaltic extrusives with a common age, as found in Phanerozoic crust (Hamilton, 2007). Instead, maps of the extent of late Archean flood basalts hint at a circular geometry (Eriksson et al., 2002) suggesting that basaltic underplating occurred over broad regions that are more circular in shape than linear. The circular geometry is consistent with Rayleigh–Taylor type instability associated with delamination and subsequent asthenospheric upwelling and decompression melting (e.g., (Elkins-Tanton, 2005).

Delamination of the mafic/ultramafic restitic lower crust by sinking through the original lithospheric mantle in Archean cratons requires that the lithospheric mantle was relatively hot and ductile (above 600–800 °C based on inferences from earthquakes (Chen and Molnar, 1983)). This inference of higher temperatures is consistent with modeling of late Archean thermal gradients in the Kaapvaal craton which predict temperatures at 40 km depth that were between 630 °C and 1010 °C for a basal mantle heat flux between 0 and 20 mW/m^2 (Gibson and Jones, 2002) and with estimates of thermal gradients of 750–1350 °C/GPa from Meso- to Neoarchean metamorphic rocks (Brown, 2007). Today the temperature at 40 km depth (i.e. Moho

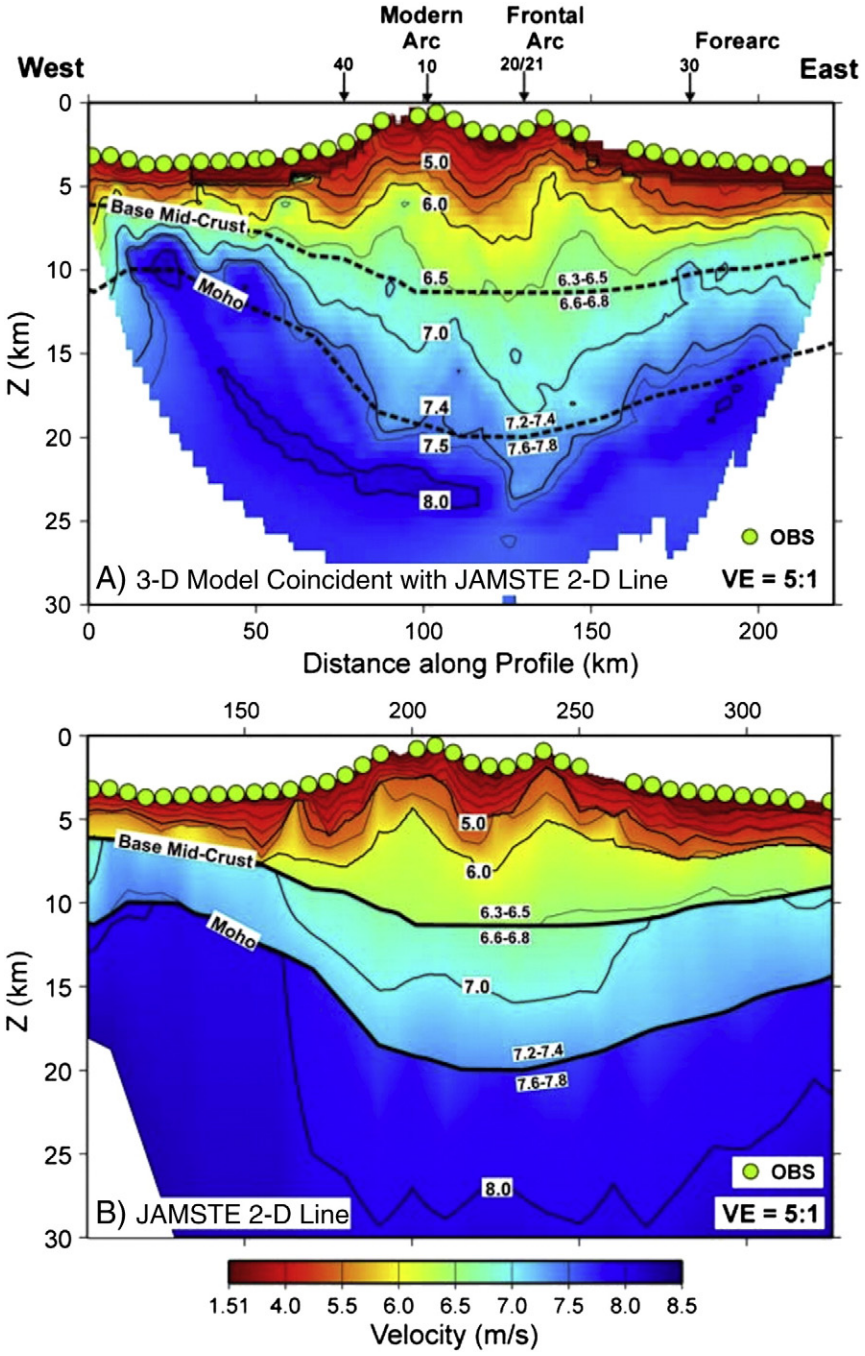

Fig. 10. Representative seismic velocity models across the Mariana arc–back–arc system from (Calvert et al., 2008). Green circles: locations of ocean bottom seismometers. Arrows: locations of seismic lines oriented perpendicular to the trend of the profile. Moho reflection is dotted black line in the top profile and solid black line in the bottom profile. (Top) Three-dimensional velocity model. (Bottom): Two dimensional velocity model. Calvert et al. (2008) note that Moho reflections are intermittent and the crustal and Moho seismic velocities are quite variable. Vertical exaggeration is 5:1.

depth) is about 350–450 °C (Artemieva and Mooney, 2001). The ductility of the lithospheric mantle and the loss of dense lower crust would have smoothed the Moho boundary, while the upper crust maintained the evidence for multiple cycles of deformation and evolving magmatic activity.

Earlier workers had a problem with large-scale delamination of basaltic–ultramafic lower crust because the ages of Archean mantle lithospheric roots were found to be approximately the same as that of the oldest granites (Pearson, 1999; Pearson et al., 1995; Shirey et al., 2004) implying that the cratonic crust and mantle formed at the same time. The ages of the lithospheric roots, however, are model ages, with potential errors of ±100 million years. Furthermore, gravity models of the Superior, Yilgarn and Pilbara cratons find that most of the mass excesses (greenstone belts) are confined to the upper crust (Nitescu and Cruden, 2006; Peschler et al., 2004) and seismic reflection data across greenstone belts confirm this conclusion (de Wit and Tinker, 2004; Drummond, 1988). Many greenstone belts are younger than surrounding granites and/or high grade metamorphic rocks (Hamilton, 2007). Finally, much less than half of the surface area of Archean cratons is composed of greenstone belts (DeWit and Ashwal, 1997). These

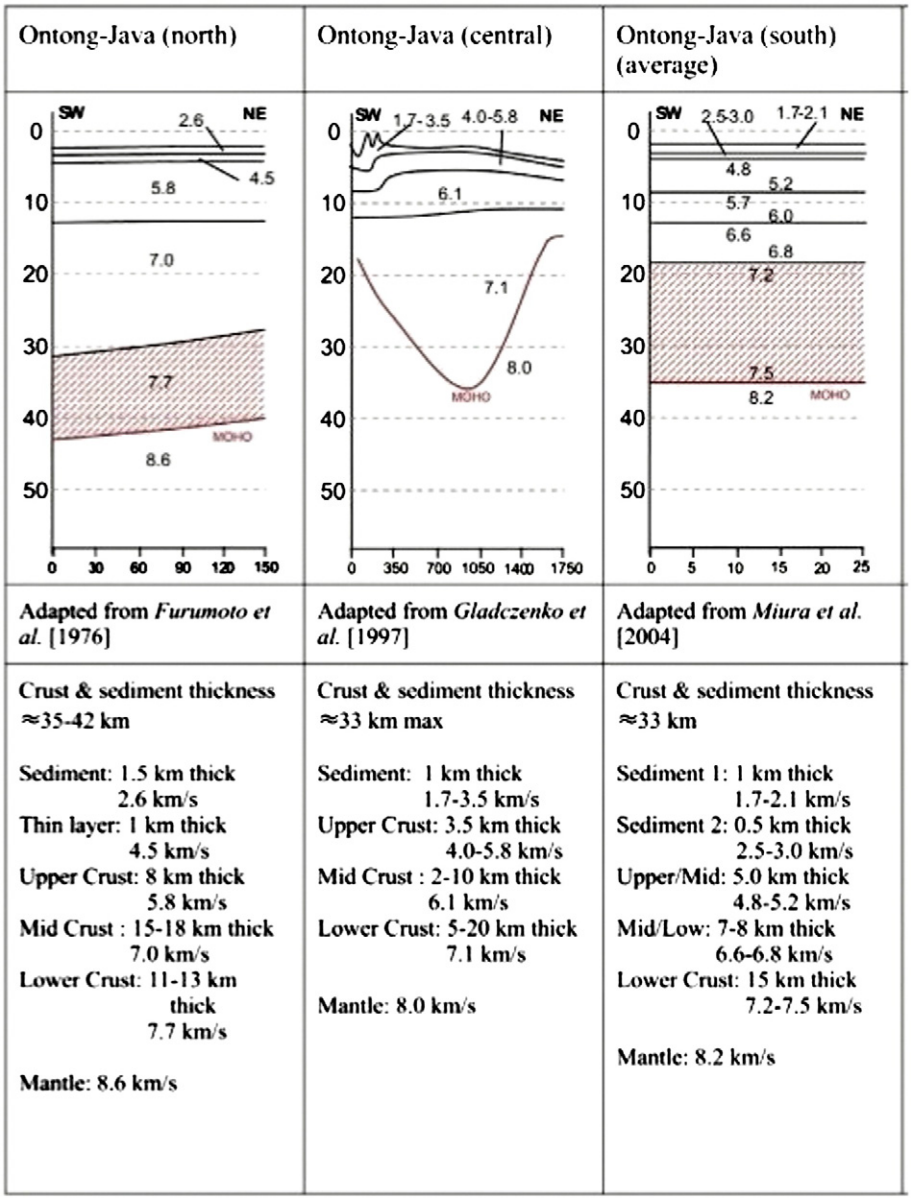

Fig. 11. Taken from compilation of (Ridley and Richards, 2010) A: after (Furumoto et al., 1976) B: after (Gladczenko et al., 1997) C: after (Miura et al., 2004).

observations coupled with seismic inferences of a silicic to intermediate lower crust imply that Archean greenstone belts do not have deep roots (Bickle et al., 1994).

Regardless of whether the lithospheric mantle remained intact during the delamination process, it is clear from the range of ages seen in the granitic suites and greenstone belts of most Archean cratons that crustal development occurred over an extended period lasting hundreds of million years or more, with multiple cycles of basaltic magmatism e.g. the Zimbabwe craton (Wilson et al., 1995). The earliest basaltic magmatism may have occurred while the crust and mantle were still sufficiently ductile and/or permeable for density differences to dominate crustal tectonics. Under these conditions, delamination could have occurred a number of times, leading to progressive geochemical evolution of the crust and ultimately the formation of the felsic tonalite–trondjehmite–granodiorite (TTG) suite (e.g. Bédard, 2006). Regardless of the exact mechanism of cratonization, a multi-stage mechanism for formation of the cratonic crust is likely.

There are still many problems that remain to be solved. The contributions of magmatic water and subduction zones to Archean magmatism are still controversial (Arndt et al., 1998; Berry et al., 2008; Parman et al., 1997). There is a continuing paradox in the preservation of thick Archean lithosphere that is as old as the oldest crust and the apparent need to add significant heat and water to multiple stages of magmatic activity during cratonic evolution over hundreds of millions of years (Schmitz and Bowring, 2003). Our research can provide constraints, but it cannot solve these problems.

12. Inferences and conclusions

Virtually all (>99%) of the Archean terranes that stabilized prior to 2.9 Ga have a sharp Moho. Around 67–74% of the Archean terranes that stabilized from 2.8 to 2.5 Ga have a sharp Moho. This could mean that there was a secular change in the process of the formation and stabilization of continental crust that was concentrated between 3.0 and 2.5 Ga.

We can explain the lack of a basaltic lower crust in undisturbed Archean terranes by early differentiation of the crust and removal of the dense restite and lower protocrust by sinking through a hotter and

more ductile lithospheric mantle (similar to that proposed by Bédard (2006) to explain the formation of Archean TTGs). The removal of the lower crust and the restite produced a sharp, flat Moho by increasing the velocity contrast between the crust and mantle due to the sinking of dense cumulates at the crust–mantle boundary. We suggest that the relative flatness of the Archean Moho was produced by removal of basaltic protocrust and restite at the depth of the garnet-in isograd (25–40 km depth, depending on bulk composition and temperature). The paucity of internal seismic discontinuities and low velocity zones in undisturbed Archean crust is probably the result of the density stratification developed during multiple intrusive events.

Acknowledgments

We thank Columbia University for access to scientific literature. We thank W. Menke for helpful discussions on the limitations of various types of seismic data. Reviews by I. M. Artemieva and N. Arndt improved the manuscript. J.V. acknowledges Jun Korenaga and the support of a Yale University Bateman Postdoctoral Fellowship and W.D.M. acknowledges discussions with K. Condie, A. Kroener, and Keith Howard, as well as support by the USGS National Earthquake Hazards Program.

References

Abbott, D., Sparks, D., Herzberg, C., Mooney, W., Nikishin, A., Zhang, Y.S., 2000. Quantifying Precambrian crustal extraction: the root is the answer. Tectonophysics 322, 163–190.
Afonso, J.C., Fernández, M., Ranalli, G., Griffin, W.L., Connolly, J.A.D., 2008. Integrated geophysical–petrological modeling of the lithosphere and sublithospheric upper mantle: methodology and applications. Geochem. Geophys. Geosyst. 9.
Alinaghi, A., Bock, G., Kind, R., Hanka, W., Wylegalla, K., 2003. Receiver function analysis of the crust and upper mantle from the North German Basin to the Archaean Baltic Shield. Geophys. J. Int. 155, 641–652.
Armstrong, R.A., Compston, W., Retief, E.A., Williams, I.S., Welke, H.J., 1991. Zircon ion microprobe studies bearing on the age and evolution of the Witwatersrand triad. Precambrian Res. 53, 243–266.
Arndt, N.T., Goldstein, S.L., 1989. An open boundary between lower continental crust and mantle: its role in crust formation and crustal recycling. Tectonophysics 161, 201–212.
Arndt, N., Ginibre, C., Chauvel, C., Albarede, F., Cheadle, M., Herzberg, C., Lahaye, Y., 1998. Were komatiites wet? Geology 26, 739–742.
Artemieva, I.M., Mooney, W.D., 2001. Thermal thickness and evolution of Precambrain lithosphere: a global study. J. Geophys. Res. 106, 16,387–316,414.
Assumpção, M., James, D., Snoke, A., 2002. Crustal thicknesses in SE Brazilian Shield by receiver function analysis: implications for isostatic compensation. J. Geophys. Res. 107. http://dx.doi.org/10.1029/2001JB000422.
Balakrishnan, S., Rajamani, V., Hanson, G.N., 1999. U–Pb ages for zircon and titanite from the Ramagiri Area, Southern India: evidence for accretionary origin of the Eastern Dharwar Craton during the Late Archean. J. Geol. 107, 69–86.
Bank, C.G., Bostock, M.G., Ellis, R.M., Cassidy, J.F., 2000. A reconnaissance teleseismic study of the upper mantle and transition zone beneath the Archaean Slave craton in NW Canada. Tectonophysics 319, 151–166.
Bédard, J.H., 2006. A catalytic delamination-driven model for coupled genesis of Archaean crust and sub-continental lithospheric mantle. Geochim. Cosmochim. Acta 70, 1188–1214.
Behn, M.D., Kelemen, P.B., 2003. Relationship between seismic P-wave velocity and the composition of anhydrous igneous and meta-igneous rocks. Geochem. Geophys. Geosyst. 4, 1041. http://dx.doi.org/10.1029/2002GC000393.
Bellucci, J.J., McDonough, W.F., Rudnick, R.L., 2011. Thermal history and origin of the Tanzanian Craton from Pb isotope thermochronology of feldspars from lower crustal xenoliths. Earth Planet. Sci. Lett. 301, 493–501.
Berry, A.J., Danyushevsky, L.V., O'Neill, H.S.C., Newville, M., Sutton, S.R., 2008. Oxidation state of iron in komatiitic melt inclusions indicates hot Archaean mantle. Nature 455, 960–963.
Bickle, M.J., Nisbet, E.G., Martin, A., 1994. Archean greenstone belts are not oceanic crust. J. Geol. 102, 121–137.
Blake, T.S., 1984. Evidence for stabilization of the Pilbara Block, Australia. Nature 307, 721–723.
Blake, T.S., 1993. Late Archaean crustal extension, sedimentary basin formation, flood basalt volcanism and continental rifting: the Nullagine and Mount Jope Supersequences, Western Australia. Precambrian Res. 60, 185–241.
Boerboom, T.J., 1994. Archean crustal xenoliths in a Keweenawan hypabyssal sill, northeastern Minnesota. White was right! Proceedings Annual Meeting, Houghton, MI. Institute on Lake Superior Geology.
Boudier, F., Nicolas, A., 1995. Nature of the Moho transition zone in the Oman ophiolite. J. Petrol. 36, 777–796.
Bowring, S.A., Williams, I.S., 1999. Priscoan (4.00 ± 4.03 Ga) orthogneisses from northwestern Canada. Contrib. Mineral. Petrol. 134, 3–16.
Bowring, S.A., Williams, I.S., Compston, W., 1989. 3.96 Ga gneisses from the Slave Province, Northwest Territories, Canada. Geology 17, 971–975.
Braile, L.W., Smith, R.B., 1975. Guide to the interpretation of seismic refraction profiles. Geophys. J. R. Astron. Soc. 40, 145–176.
Brown, M., 2007. Metamorphic conditions in orogenic belts: a record of secular change. Int. Geol. Rev. 49, 193–234.
Calvert, A.J., Sawyer, E.W., Davis, W.J., Ludden, J.N., 1995. Archaean subduction inferred from seismic images of a mantle suture in the Superior Province. Nature 375, 670–674.
Calvert, A.J., Klemperer, S.L., Takahashi, N., Kerr, B.C., 2008. Three-dimensional crustal structure of the Mariana island arc from seismic tomography. J. Geophys. Res. 113, B01406. http://dx.doi.org/10.1029/02007JB004939.
Card, K.D., 1990. A review of the Superior Province of the Canadian Shield, a product of Archean accretion. Precambrian Res. 48, 99–156.
Chen, W.P., Molnar, P., 1983. Focal depths of intracontinental and intraplate earthquakes and their implications for the thermal and mechanical properties of the lithosphere. J. Geophys. Res. 88, 4183–4214.
Chen, Y., Niu, F., Liu, R., Huang, Z., Tkalcic, H., Sun, L., Chan, W., 2010. Crustal structure beneath China from receiver function analysis. J. Geophys. Res. 115. http://dx.doi.org/10.1029/2009JB006386.
Chown, E.H., Harrap, R., Moukhsil, A., 2002. The role of granitic intrusions in the evolution of the Abitibi belt, Canada. Precambrian Res. 115, 291–310.
Christensen, N.I., Mooney, W.D., 1995. Seismic velocity structure and composition of the continental crust: a global view. J. Geophys. Res. 100, 9761–9788.
Collins, J.A., Brocher, T.M., Karson, J.A., 1986. Two-dimensional seismic reflection modeling of the inferred fossil oceanic crust/mantle transition in the Bay of Islands Ophiolite. J. Geophys. Res. 91, 12520–12538.
Compston, W., Kröner, A., 1988. Multiple zircon growth within early Archaean tonalitic gneiss from the Ancient Gneiss Complex, Swaziland. Earth Planet. Sci. Lett. 87, 13–28.
Condie, K.C., 1999. Mafic crustal xenoliths and the origin of the lower continental crust. Lithos 46, 95–101.
Condie, K.C., 2005. High field strength element ratios in Archean basalts: a window to evolving sources of mantle plumes? Lithos 79, 491–504.
Connelly, J.N., Ryan, B., 1996. Late Archean evolution of the Nain Province, Nain, Labrador: imprint of a collision. Can. J. Earth Sci. 33, 1325–1342.
Cook, F.A., 2002. Fine structure of the continental reflection Moho. Geol. Soc. Am. Bull. 114, 64–79.
Cook, F.A., White, D.J., Jones, A.G., Eaton, D.W.S., Hall, J., Clowes, R.M., 2010. How the crust meets the mantle: lithoprobe perspectives on the Mohorovicic discontinuity and crust–mantle transition. Can. J. Earth Sci. 47, 315–351.
Corcoran, P.L., 2012. Archaean sedimentary sequences of the Slave craton. Mar. Pet. Geol. 33, 80–91.
Corfu, F., 1996. Multistage zircon and titanite growth and inheritance in an Archean gneiss complex, Winnipeg River Subprovince, Ontario. Earth Planet. Sci. Lett. 141, 175–186.
Corfu, F., Stott, G.M., 1993. Age and petrogenesis of two late Archean magmatic suites, northwestern Superior Province, Canada: zircon U–Pb and Lu–Hf isotopic relations. J. Petrol. 34, 817–838.
Czarnota, K., Champion, D.C., Goscombe, B., Blewett, R.S., Cassidy, K.F., Henson, P.A., Groenewald, P.B., 2010. Geodynamics of the eastern Yilgarn Craton. Precambrian Res. 183, 175–202.
Darbyshire, F.A., Eaton, D.W., Fredericksen, A.W., Ertolahti, L., 2007. New insights into the lithosphere beneath the Superior Province from Rayleigh wave dispersion and reciever function analysis. Geophys. J. Int. 169, 1043–1068.
Davis, D.W., 2002. U–Pb geochronology of Archean metasedimentary rocks in the Pontiac and Abitibi subprovinces, Quebec, constraints on timing, provenance and regional tectonics. Precambrian Res. 115, 97–117.
Davis, D.W., Amelin, Y., Nowell, G.M., Parrish, R.R., 2005. Hf isotopes in zircon from the western Superior province, Canada: implications for Archean crustal development and evolution of the depleted mantle reservoir. Precambrian Res. 140, 132–156.
de Wit, M., Tinker, J., 2004. Crustal structures across the central Kaapvaal craton from deep-seismic reflection data. S. Afr. J. Geol. 107, 185–206.
De Wit, M.J., Roering, C., Hart, R.J., Armstrong, R.A., De Ronde, C.E.J., Green, R.W.E., Tredoux, M., Peberdy, E., Hart, R.A., 1992. Formation of an Archaean continent. Nature 357, 553–562.
DeWit, M.J., Ashwal, L., 1997. Greenstone Belts. Oxford Monographs on Geology and GeophysicsOxford University Press.
deWit, M.J., Roering, C., Hart, R.J., Armstrong, R.A., Ronde, C.E.J.d, Green, R.W.E., Tredoux, M., Peberdy, E., Hart, R.A., 1992. Formation of an Archean continent. Nature 357, 553–562.
Dodson, M.H., Compston, W., Williams, I.S., Wilson, J.F., 1988. A search for ancient detrital zircons in southern Zimbabwe. J. Geol. Soc. Lond. 145, 977–983.
Dodson, M.H., Williams, I.S., Kramers, J.D., 2001. The Mushandike granite: further evidence for 3.4 Ga magmatism in the Zimbabwe craton. Geol. Mag. 138, 31–38.
Drummond, B.J., 1988. A review of crust/upper mantle structure in the Precambrian areas of Australia and implications of Precambrian crustal evolution. Precambrian Res. 40–41, 101–116.
Drummond, B.J., Goleby, B.R., Swager, C.P., 2000. Crustal signature of Late Archaean tectonic episodes in the Yilgarn craton, Western Australia: evidence from deep seismic sounding. Tectonophysics 329 (2000), 193–221.
Durrheim, R.J., Green, R.W.E., 1992. A seismic refraction investigation of the Archean Kaapvaal Craton, South Africa, using mine tremors as an energy source. Geophys. J. Int. 108, 812–832.
Durrheim, R.J., Mooney, W.D., 1991. Archean and Proterozoic crustal evolution: evidence from crustal seismology. Geology 19, 606–609.
Durrheim, R.J., Mooney, W.D., 1994. Evolution of the Precambrian lithosphere: seismological and geochemical constraints. J. Geophys. Res. 99, 15359–15374.

Elkins-Tanton, L.T., 2005. Continental magmatism caused by lithospheric delamination. In: Foulger, G.R. (Ed.), Plumes, Plates and Paradigms, vol. 388. Geological Society of America, Denver, CO, pp. 449–462.
Eriksson, K.A., Donaldson, J.A., 1986. Basinal and shelf sedimentation in relation to the Archaean–Proterozoic boundary. Precambrian Res. 33, 103–121.
Eriksson, K.A., Fedo, C.M., 1994. Archean synrift and stable-shelf sedimentary successions. In: Condie, K. (Ed.), Developments in Precambrian Geology, vol. 11. Elsevier, pp. 171–204.
Eriksson, P.G., Condie, K.C., Westhuizen, W.V.D., Merwe, R.V.D., Bruiyn, H.D., Nelson, D.R., Cunningham, M.J., 2002. Late Archaean superplume events: a Kaapvaal–Pilbara perspective. J. Geodyn. 34, 207–247.
Fedo, C.M., Sircombe, K.N., Rainbird, R.H., 2003. Detrital zircon analysis of the sedimentary record. Rev. Mineral. Geochem. 53, 277–303.
Fernández Viejo, G., Clowes, R.M., 2003. Lithospheric structure beneath the Archaean Slave Province and Proterozoic Wopmay orogen, northwestern Canada, from a LITHOPROBE refraction/wide-angle reflection survey. Geophys. J. Int. 153, 1–19.
Fountain, D.M., Christensen, N.I., 1989. Composition of the continental crust and upper mantle; a review. In: Pakiser, L.C., Mooney, W.D. (Eds.), Geophysical Framework of the Continental United States, vol. Memoire 172. Geological Society of America, pp. 711–742.
Friend, C.R., Nutman, A.P., Baadsgaard, H., Duke, M.J.M., 2009. The whole rock Sm–Nd 'age'for the 2825 Ma Ikkattoq gneisses (Greenland) is 800 Ma too young: insights into Archaean TTG petrogenesis. Chem. Geol. 261, 62–76.
Funck, T., Hansen, A., Reid, I.D., Louden, K.E., 2008. The crustal structure of the southern Nain and Makkovik provinces of Labrador derived from refraction seismic data. Can. J. Earth Sci. 45, 465–481.
Furumoto, A.S., Webb, J.P., Odegard, M.E., Hussong, D.M., 1976. Seismic studies on the Ontong Java Plateau. Tectonophysics 34, 71–90.
Geng, Y., Du, L., Ren, L., 2012. Growth and reworking of the early Precambrian continental crust in the North China Craton: constraints from zircon Hf isotopes. Gondwana Res. 21, 517–529.
Gibson, R.L., Jones, M.Q.W., 2002. Late Archean to Paleoproterozoic geotherms in the Kaapvaal craton, South Africa: constraints on the thermal evolution of the Witwatersrand basin. Basin Res. 14, 169–181.
Gladczenko, T.P., Coffin, M.F., Eldholm, O., 1997. Crustal structure of the Ontong Java Plateau: modeling of new gravity and existing seismic data. J. Geophys. Res. 102, 22,711–722,729.
Gorbatschev, R., Bogdanova, S., 1993. Frontiers in the Baltic shield. Precambrian Res. 64, 3–21.
Gore, J., James, D.E., Zengeni, T.G., Gwavava, O., 2009. Crustal structure of the Zimbabwe craton and the Limpopo belt of Southern Africa: new constraints from seismic data and implications for its evolution. S. Afr. J. Geol. 112, 213–228.
Grandjean, G., Wu, H., White, D., Mareschal, M., Hubert, C., 1995. Crustal velocity models for the Archean Abitibi greenstone belt from seismic refraction data. Can. J. Earth Sci. 32, 149–166.
Griffin, W.L., O'Reilly, S.Y., 1987. The composition of the lower crust and the nature of the continental Moho–xenoliths evidence. In: Nixon, P.H. (Ed.), Mantle Xenoliths. Wiley, Chichester, UK, pp. 413–432.
Griffin, W.L., Belousova, E.A., Shee, S.R., 2004. Archean crustal evolution in the northern Yilgarn Craton: U–Pb and Hf-isotope evidence from detrital zircons. Precambrian Res. 131, 231–282.
Hale, L.D., Thompson, G.A., 1982. The seismic reflection character of the continental Mohorovičić discontinuity. J. Geophys. Res. 87, 4625–4635.
Hamilton, W.B., 2007. Earth's first two billion years—the era of internally mobile crust. In: Hatcher Jr., R.D., Carlson, M.P., McBride, J.H., Catalan, J.R.M. (Eds.), 4-D Framework of Continental Crust, vol. Memoir 200. Geological Society of America, Denver, CO.
Han, B.F., Xu, Z., Ren, R., Li, L.L., Yang, J.H., Yang, Y.H., 2012. Crustal growth and intracrustal recycling in the middle segment of the Trans-North China Orogen, North China Craton: a case study of the Fuping Complex. Geol. Mag. 149, 729–742.
Hansen, G.N., 1975. 40Ar/39Ar Spectrum Ages on Logan Intrusions, a Lower Keweenawan Flow, and Mafic Dikes in Northeastern Minnesota—Northwestern Ontario. Can. J. Earth Sci. 12, 821–835.
Hartlaub, R.P., Heaman, L.M., Ashton, K.E., Chacko, T., 2004. The Archean Murmac Bay Group: evidence for a giant archean rift in the Rae Province, Canada. Precambrian Res. 131, 345–372.
Hartlaub, R.P., Chacko, T., Heaman, L.M., Creaser, R.A., Ashton, K.E., Simonetti, A., 2005. Ancient (Meso-to Paleoarchean) crust in the Rae Province, Canada: evidence from Sm–Nd and U–Pb constraints. Precambrian Res. 141, 137–153.
Hartmann, L.A., Endo, I., Suita, M.T.F., Santos, J.O.S., Frantz, J.C., Carneiro, M.A., Barley, M.E., 2006. Provenance and age delimitation of Quadrilátero Ferrífero sandstones based on zircon U–Pb isotopes. J. S. Am. Earth Sci. 20, 273–285.
Hegner, E., Kröner, A., Hunt, P., 1994. A precise U_Pb zircon age for the Archaean Pongola Supergroup volcanics in Swaziland. J. Afr. Earth Sci. 18, 339–341.
Helmstaedt, H.L., 2009. Crust–mantle coupling revisited: the Archean Slave craton, NWT, Canada. Lithos 112, 1055–1068.
Helmstaedt, H., 2010. Ages of cratonic diamonds and lithosphere evolution: constraints on Precambrian tectonics and diamond exploration. Can. Mineral. 48, 1385–1408.
Henry, P., Stevenson, R.K., Larbi, Y., Gariépy, C., 2000. Nd isotopic evidence for early to late Archean (3.4–2.7 Ga) crustal growth in the Western Superior Province (Ontario, Canada). Tectonophysics 322, 135–151.
Herzberg, C., Rudnick, R., 2012. Formation of cratonic lithosphere: an integrated thermal and petrological model. Lithos 149, 4–15 (*esearch*, 231, 174-193).
Herzberg, C., Condie, C., Korenaga, J., 2010. Thermal history of the Earth and its petrological expression. Earth Planet. Sci. Lett. 292, 79–88.
Hoffman, P.F., 1988. United Plates of America, the birth of a craton—Early Proterozoic assembly and growth of Laurentia. Annual Review of Earth and Planetary Sciences 16, 543–603.
Holbrook, W.S., Mooney, W.D., Christensen, N.I., 1992. The seismic velocity structure of the deep continental crust. In: Fountain, D.M., Arculus, R., Kay, R. (Eds.), Continental Lower Crust. Elsevier, Amsterdam, pp. 1–43.
Horstwood, M.S.A., Nesbitt, R.W., Noble, S.R., Wilson, J.F., 1999. U–Pb zircon evidence for an extensive early Archean craton in Zimbabwe: a reassessment of the timing of craton formation. Geology 27, 707–710.
Ivanic, T.J., Van Kranendonk, M.J., Kirkland, C.L., Wyche, S., Wingate, M.T., Belousova, E.A., 2012. Zircon Lu–Hf isotopes and granite geochemistry of the Murchison Domain of the Yilgarn Craton: evidence for reworking of Eoarchean crust during Meso-Neoarchean plume-driven magmatism. Lithos 148, 112–127.
Jagoutz, O., Schmidt, M., 2012. The formation and bulk composition of modern juvenile continental crust: the Kohistan arc. Chem. Geol. 298–299, 79–96.
Jagoutz, O., Müntener, O., Schmidt, M.W., Burg, J.P., 2011. The roles of flux- and decompression melting and their respective fractionation lines for continental crust formation: evidence from the Kohistan arc. Earth Planet. Sci. Lett. 303, 25–36.
James, D.T., Kamo, S., Krogh, T., 2002. Evolution of 3.1 and 3.0 Ga volcanic belts and a new thermotectonic model for the Hopedale Block, North Atlantic craton (Canada). Canadian Journal of Earth Sciences 39, 687–710.
James, D.E., Niu, F., Rokosky, J., 2003. Crustal structure of the Kaapvaal craton and its significance for early crustal evolution. Lithos 71, 413–429.
Jarchow, C.M., Thompson, G.A., 1989. The nature of the Mohorovicic discontinuity. Annual Review of Earth and Planetary Science 17, 475–506.
Kabete, J.M., McNaughton, N.J., Groves, D.I., Mruma, A.H., 2012. Reconnaissance SHRIMP U–Pb zircon geochronology of the Tanzania Craton: evidence for Neoarchean granitoid-greenstone belts in the Central Tanzania Region and the Southern East African Orogen. Precambrian Research 216–219, 232–266.
Kaur, P., Zeh, A., Chaudhri, N., Gerdes, A., Okrusch, M., 2011. Archaean to Palaeoproterozoic crustal evolution of the Aravalli mountain range, NW India, and its hinterland: the U–Pb and Hf isotope record of detrital zircon. Precambrian Research 187, 155–164.
Kay, R.W., Mahlburg Kay, S., 1983. Delamination and delamination magmatism. Tectonophysics 219, 177–189.
Kgaswane, E.M., Nyblade, A.A., Julià, J., Dirks, P.H., Durrheim, R.J., Pasyanos, M.E., 2009. Shear wave velocity structure of the lower crust in southern Africa: evidence for compositional heterogeneity within Archaean and Proterozoic terrains. J. Geophys. Res. 114, B12304-.
Kodaira, S., Noguchi, N., Takahashi, N., Ishizuka, O., Kaneda, Y., 2010. Evolution from fore-arc oceanic crust to island arc crust: a seismic study along the Izu–Bonin fore arc. J. Geophys. Res. 115. http://dx.doi.org/10.1029/2009JB006968.
Kozlovskaya, E., Kosarev, G., Aleshin, I., Riznichenko, O., Sanina, I., 2008. Structure and composition of the crust and upper mantle of the Archean–Proterozoic boundary in the Fennoscandian shield obtained by joint inversion of receiver function and surface wave phase velocity of recording of the SVEKALAPKO array. Geophys. J. Int. 175, 135–152.
Kumar, P., Kind, R., Priestley, K., Dahl-Jensen, T., 2007. Crustal structure of Iceland and Greenland from receiver function studies. J. Geophys. Res. 112. http://dx.doi.org/10.1029/2005JB003991.
Kumar, T.J., Jagadeesh, S., Rai, S.S., 2012. Crustal structure beneath the Archean–Proterozoic terrain of north India from receiver function modeling. Journal of Asian Earth Sciences 58, 108–118.
Last, R.J., Nyblade, N.A., Langston, C.A., Owens, T.J., 1997. Crustal structure of the African Plateau from reciever functions and Raleigh wave phase velocities. J. Geophys. Res. 102, 24, 469–24, 483.
Lauri, L.S., Andersen, T., Hölttä, P., Huhma, H., Graham, S., 2011. Evolution of the Archaean Karelian Province in the Fennoscandian Shield in the light of U–Pb zircon ages and Sm–Nd and Lu–Hf isotope systematics. J. Geol. Soc. 168, 201–218.
Lawley, C.J., Selby, D., Condon, D.J., Horstwood, M., Millar, I., Crowley, Q., Imber, J., 2013. Lithogeochemistry, geochronology and geodynamic setting of the Lupa Terrane, Tanzania: implications for the extent of the Archean Tanzanian craton. Precambrian Res. 231, 174–193.
Liu, D.Y., Nutman, A.P., Compston, W., Wu, J.S., Shen, Q.H., 1992. Remnants of 3800 Ma crust in the Chinese part of the Sino-Korean craton. Geology 20, 339–342.
Louden, K.E., Fan, J., 1988. Crustal structures of Grenville, Makkovik, and southern Nain provinces along the Lithoprobe ECSOOT Transect: regional seismic refraction and gravity models and their tectonic implications. Can. J. Earth Sci. 35, 583–601.
Lowe, D.R., 1980. Archean sedimentation. Ann. Rev. Earth Planet. Sci. 8, 145–167.
Ma, M., Wan, Y., Santosh, M., Xu, Z., Xie, H., Dong, C., Guo, C., 2012. Decoding multiple tectonothermal events in zircons from single rock samples: SHRIMP zircon U–Pb data from the late Neoarchean rocks of Daqingshan, North China Craton. Gondwana Res. 22 (3), 810–827.
Mall, D.M., Chandrakala, K., Kumar, A.S., Sarkar, D., 2012. Sub-crustal LVZ below Dharwar craton, India: an evidence for remobilization of Archean crust. Precambrian Res. 206–211, 161–173.
Mänttäri, I., Hölttä, P., 2002. U–Pb dating of zircons and monazites from Archean granulites in Varpaisjärvi, Central Finland: evidence for multiple metamorphism and Neoarchean terrane accretion. Precambrian Res. 118, 101–131.
Meert, J.G., Pandit, M.K., Pradhan, V.R., Banks, J., Sirianni, R., Stroud, M., Gifford, J., 2010. Precambrian crustal evolution of Peninsular India: a 3.0 billion year odyssey. J. Asian Earth Sci. 39, 483–515.
Mikkola, P., Huhma, H., Heilimo, E., Whitehouse, M., 2011. Archean crustal evolution of the Suomussalmi district as part of the Kianta Complex, Karelia: constraints from geochemistry and isotopes of granitoids. Lithos 125, 287–307.
Miller, M.S., Eaton, D.W., 2010. Formation of cratonic mantle keels by arc accretion: evidence from S receiver functions. Geophys. Res. Lett. 37.

Mints, M., Suleimanov, A., Zamozhniaya, N., Stupak, V., 2009. A three-dimensional model of the Early Precambrian crust under the southeastern Fennoscandian Shield: Karelia craton and Belomorian tectonic province. Tectonophysics 472, 323–339.
Miura, S., Suyehiro, K., Shinohara, M., Takahashi, N., Araki, E., Taira, A., 2004. Seismological structure and implications of collision between the Ontong Java Plateau and Solomon Island Arc from ocean bottom seismometer–airgun data. Tectonophysics 389, 191–220.
Mooney, W.D., 1989. Seismic methods for determining earthquake source parameters and lithospheric structure. In: Pakiser, L.C., Mooney, W.D. (Eds.), Geophysical Framework of the Continental United States, vol. G.S.A. Memoir 172, pp. 11–34.
Mooney, W.D., Brocher, T.M., 1987. Coincident seismic reflection/refraction studies of the continental lithosphere: a global review. Geophys. J. Int. 89, 1–6.
Mooney, W.D., Meissner, R., 1992. Multi-genetic origin of crustal reflectivity: a review of seismic reflection profiling of the continental lower crust and Moho: continental lower crust. Dev. Geotecton. 23, 45–79.
Mooney, W.D., Laske, G., Masters, G., 1998. CRUST 5.1: a global crustal model at 5 degrees × 5 degrees. J. Geophys. Res. 103, 727–747.
Moorbath, S., Taylor, P.N., Orpen, J.L., Treloar, P., Wilson, J.F., 1987. First direct radiometric dating of Archaean stromatolitic limestone. Nature 326, 865–867.
Moser, D.E., Flowers, R.M., Hart, R.J., 2001. Birth of the Kaapvaal tectosphere 3.08 billion years ago. Science 291, 465–468.
Musacchio, G., White, D.J., Asudeh, I., Thomson, C., 2004. Lithospheric structure and composition of the Archean western Superior Province from seismic refraction/wide-angle reflection and gravity modeling. J. Geophys. Res. 109, B03304.
Nägler, T.F., Kramers, J.D., Kamber, B.S., Frei, R., Prendergast, M.D.A., 1997. Growth of subcontinental lithospheric mantle beneath Zimbabwe started at or before 3.8 Ga: Re–Os study on chromites. Geology 25, 983–986.
Naha, K., Srinivasan, R., Gopalan, K., Pantulu, G.V.C., Rao, S., Vrevsky, A.B., Bogomolov, Y.S., 1993. The nature of the basement in the Archaean Dharwar craton of southern India and the age of the Peninsular Gneiss. Proc. Indian Acad. Sci. Earth Planet. Sci. 102, 547–565.
Nair, S.K., Gao, S.S., Liu, K.H., Sllver, P.G., 2006. Southern African crustal evolution and composition: constraints from receiver function studies. J. Geophys. Res. 111, B02304. http://dx.doi.org/10.1029/2005JB003802.
Nguuri, T.K., Gore, J., James, D.E., Webb, S.J., Wright, C., Zengeni, T.G., Gwavava, O., Snoke, J.A., Group, K.S., 2001. Crustal structure beneath southern Africa and its implications for the formation and evolution of the Kaapvaal and Zimbabwe cratons. Geophys. Res. Lett. 28, 2501–2504.
Nitescu, B., Cruden, A.R., 2006. Crustal structure and implications for the tectonic evolution of the Archean Western Superior craton from forward and inverse gravity modeling. Tectonics 25, TC1009.
Niu, F., James, D.E., 2002. Fine structure of the lowermost crust beneath the Kaapvaal craton and its implications for crustal formation and evolution. Earth Planet. Sci. Lett. 200, 121–130.
Nutman, A.P., Friend, C.R., 2007. Adjacent terranes with ca. 2715 and 2650 Ma high-pressure metamorphic assemblages in the Nuuk region of the North Atlantic Craton, southern West Greenland: complexities of Neoarchaean collisional orogeny. Precambrian Res. 155, 159–203.
Nutman, A.P., Chadwick, B., Ramakrishnan, M., Viswanathan, M.N., 1992. SHRIMP U–Pb ages of detrital zircon in Sargur supracrustal rocks in western Karnataka, southern India. J. Geol. Soc. India 39, 367–374.
Nutman, A.P., Bennett, V.C., Friend, C.R., Horie, K., Hidaka, H., 2007. <3,850 Ma tonalites in the Nuuk region, Greenland: geochemistry and their reworking within an Eoarchaean gneiss complex. Contrib. Mineral. Petrol. 154, 385–408.
Nutman, A.P., Friend, C.R., Paxton, S., 2009. Detrital zircon sedimentary provenance ages for the Eoarchaean Isua supracrustal belt southern West Greenland: juxtaposition of an imbricated ca. 3700 Ma juvenile arc against an older complex with 3920–3760 Ma components. Precambrian Res. 172, 212–233.
O'Neil, J., Maurice, C., Stevenson, R.K., Larocque, J., Cloquet, C., David, J., Francis, D., 2007. The Geology of the 3.8 Ga Nuvvuagittuq (Porpoise Cove) Greenstone Belt, Northeastern Superior Province, Canada. In: Condie, K. (Ed.), Developments in Precambrian Geology, vol. 15. Elsevier, pp. 219–250.
Parman, S.W., Dann, J.C., Grove, T.L., De Wit, M.J., 1997. Emplacement conditions of komatiite magmas from the 3.49 Ga Komati Formation, Barberton greenstone belt, South Africa. Earth Planet. Sci. Lett. 150, 303–323.
Pearson, D.G., 1999. The age of continental roots. Lithos 48, 171–194.
Pearson, D.G., Carlson, R.W., Shirey, S.B., Boyd, F.R., Nixon, P.H., 1995. Stabilisation of Archaean lithospheric mantle: a Re–Os isotope study of peridotite xenoliths from the Kaapvaal craton. Earth Planet. Sci. Lett. 134, 341–357.
Peschler, A.P., Benn, K., Roest, W.R., 2004. Insights on Archean continental geodynamics from gravity modelling of granite-greenstone terranes. J. Geodyn. 38, 185–207.
Peucat, J.J., Figueiredo Barbosa, J.S., Conceição de Araújo Pinho, I., Paquette, J.L., Martin, H., Fanning, C.M., Cruz, S., 2011. Geochronology of granulites from the south Itabuna-Salvador-Curaçá Block, São Francisco Craton (Brazil): Nd isotopes and U–Pb zircon ages. J. S. Am. Earth Sci. 31, 397–413.
Reading, A.M., Kennett, B.L.N., 2003. Lithospheric structure of the Pilbara Craton, Capricorn Orogen and northern Yilgarn Craton, Western Australia, from teleseismic receiver functions. Aust. J. Earth Sci. 50, 439–445.
Reading, A.M., Tkalčić, H., Kennett, B.L.N., Johnson, S.P., Sheppard, S., 2012. Seismic structure of the crust and uppermost mantle of the Capricorn and Paterson Orogens and adjacent cratons, Western Australia, from passive seismic transects. Precambrian Res. 196–197, 295–308.
Ridley, V.A., Richards, M.A., 2010. Deep crustal structure beneath large igneous provinces and the petrologic evolution of flood basalts. Geochem. Geophys. Geosyst. 11, GC002935.
Rios, D.C., Davis, D.W., Conceição, H., Macambira, M.J.B., Peixoto, A.A., Oliveira, L.L., 2008. Ages of granites of the Serrinha Nucleus, Bahia (Brazil): an overview. Rev. Bras. Geosci. 30, 74–77.
Rollinson, H., 2010. Coupled evolution of Archean continental crust and subcontinental lithospheric mantle. Geology 38, 1083–1086.
Roy, A.B., Kröner, A., 1996. Single zircon evaporation ages constraining the growth of the Archaean Aravalli craton, northwestern Indian shield. Geol. Mag. 133, 333–342.
Roy, A.B., Kröner, A., Bhattachaya, P.K., Rathore, S., 2005. Metamorphic evolution and zircon geochronology of early Proterozoic granulites in the Aravalli Mountains of northwestern India. Geol. Mag. 142, 287–302.
Rudnick, R.L., Fountain, D.M., 1995. Nature and composition of the continental crust: a lower crustal perspective. Rev. Geophys. 33, 267–310.
Rudnick, R.L., Gao, S., 2003. Composition of the continental crust. In: Rudnick, R.L. (Ed.), The Crust, vol. 3. Elsevier-Pergamon, Oxford, pp. 1–64.
Sandeman, H.A., Hanmer, S., Davis, W.J., Ryan, J.J., Peterson, T.D., 2004. Neoarchaean volcanic rocks, Central Hearne supracrustal belt, Western Churchill Province, Canada: geochemical and isotopic evidence supporting intra-oceanic, supra-subduction zone extension. Precambrian Res. 134, 113–141.
Sandeman, H.A., Schultz, M., Rubingh, K., 2005. Results of Bedrock Mapping of the Darby Lake-Arrowsmith River North Map Areas. Nunavut Geological Survey of Canada, Central Rae Domain.
Sasseville, C., Tomlinson, K.Y., Hynes, A., McNicoll, V., 2006. Stratigraphy, structure, and geochronology of the 3.0 2.7 Ga Wallace Lake greenstone belt, western Superior Province, southeast Manitoba. Can. J. Earth Sci. 43, 929–945.
Schiøtte, L., Compston, W., Bridgwater, D., 1989. U–Th–Pb ages of single zircons in Archaean supracrustals from Nain Province, Labrador, Canada. Can. J. Earth Sci. 26, 2636–2644.
Schiøtte, L., Hansen, B.T., Shirey, S.B., Bridgwater, D., 1993. Petrological and whole rock isotopic characteristics of tectonically juxtaposed Archaean gneisses in the Okak area of the Nain Province, Labrador: relevance for terrane models. Precambrian Res. 63, 293–323.
Schmitz, M.D., Bowring, S.A., 2003. Ultrahigh-temperature metamorphism in the lower crust during Neoarchean Ventersdorp rifting and magmatism. Geol. Soc. Am. Bull. 115, 533–548.
Schoene, B., Dudas, F.O., Bowring, S.A., De Wit, M., 2009. Sm–Nd isotopic mapping of lithospheric growth and stabilization in the eastern Kaapvaal craton. Terra Nova 21, 219–228.
Schulze, D.J., 1989. Constraints on the abundance of eclogite in the upper mantle. J. Geophys. Res. 94, 4205–4212.
Shirey, S.B., Richardson, S.H., 2011. Start of the Wilson cycle at 3 Ga shown by diamonds from subcontinental mantle. Science 333, 434–436.
Shirey, S.B., Richardson, S.H., Harris, J.W., 2004. Integrated models of diamond formation and craton evolution. Lithos 77, 923–944.
Slabunov, A.I., Lobach-Zhuchenko, S.B., Bibikova, E.V., Sorjonen-Ward, P., Balangansky, V.V., Volodichev, O.I., Stepanov, V.S., 2006. The Archaean nucleus of the Fennoscandian (Baltic) Shield. Geol. Soc. London Mem. 32, 627–644.
Smithies, R.H., Champion, D.C., van Kranendonk, M.J., 2009. Formation of Paleoarchean continental crust through infracrustal melting of enriched basalt. Earth Planet. Sci. Lett. 281, 298–306.
Song, B., Nutman, A.P., Liu, D.Y., Wi, J.S., 1996. 3800 to 2500 Ma crustal evolution in the Anshan area of Liaoning Province, northeastern China. Precambrian Res. 78, 79–94 (Precambrian Research, v. 78, p. 79–94).
Stein, S., Wysession, M., 2003. An Introduction to Seismology, Earthquakes and Earth Structure. Blackwell Publishing, Padstow, Cornwall, UK (498 pp.).
Steinhart, J., 1967. Mohorovic discontinuity. In: Runcorn, S.K. (Ed.), International Dictionary of Geophysics, vol. 2. Pergamon Press, Oxford, UK, pp. 991–994.
Stern, R.A., Bleeker, W., 1988. Age of the worlds oldest rocks refined using Canada's SHRIMP: the Acasta Gneiss Complex, NW Territories, Canada. Geoscience Canada 25, 27–31.
Takahashi, N., Kodaira, S., Tatsumi, Y., Kaneda, Y., Suyehiro, K., 2008. Structure and growth of the Izu-Bonin-Mariana arc crust: 1. Seismic constraint on crust and mantle structure of the Mariana arc–back–arc system. J. Geophys. Res. 113, B01104.
Taylor, S.R., McLennan, S.M., 1985. The Continental Crust: Its Composition and Evolution. Blackwell Scientific Publications, Palo Alto, CA (328 pp.).
Taylor, S.R., McLennan, S.J., 1995. The geochemical evolution of the continental crust. Rev. Geophys. 33, 241–265.
Thern, E.R., Nelson, D.R., 2012. Detrital zircon age structure within ca. 3 Ga metasedimentary rocks, Yilgarn Craton: elucidation of Hadean source terranes by principal component analysis. Precambrian Res. 214–215, 28–43.
Thompson, D.A., Bastow, I.D., Helffrich, G., Kendall, J.-M., Wookey, J., Snyder, D.B., Eaton, D.W., 2010. Precambrian crustal evolution: seismic constraints from the Canadian Shield. Earth Planet. Sci. Lett. 297, 655–656.
Thorpe, R.I., Hickman, A., Davis, D.W., Mortensen, J.K., Trendall, A.F., 1992. U/Pb zircon geochronology of Archaean felsic units in the Marble Bar region, Pilbara Craton, Western Australia. Precambrian Res. 56, 169–189.
Tomlinson, K.Y., Stott, G.M., Percival, J.A., Stone, D., 2004. Basement terrane correlations and crustal recycling in the western Superior Province: Nd isotopic character of granitoid and felsic volcanic rocks in the Wabigoon subprovince, N. Ontario. Precambrian Res. 132, 245–274.
Tugame, F., Nyblade, A., Julia, J., 2012. Moho depths and Poisson's ratios of Precambrian crust in East Africa: evidence for similarities in Archean and Proterozoic crustal structure. Earth Planet. Sci. Lett. 355–356, 73–81.
van Breemen, O., Harper, C.T., Berman, R.G., Wodicka, N., 2007. Crustal evolution and Neoarchean assembly of the central-southern Hearne domains: evidence from U–Pb geochronology and Sm–Nd isotopes of the Phelps Lake area, northeastern Saskatchewan. Precambrian Res. 159, 33–59.

Van Kranendonk, M.J., Smithies, H.R., Hickman, A.H., Champion, D.C., 2007. Review: secular tectonic evolution of Archean continental crust: interplay between horizontal and vertical processes in the formation of the Pilbara Craton, Australia. Terra Nova 19, 1–38.
Vantongeren, J., Korenaga, J., 2012. Phase relations and density considerations in a thick (>25 km) Archean "oceanic" crust, 34th IGC, Volume Abstract. IGC, Brisbane, Australia 205.
Vera, E.E., Mutter, J.C., Buhl, P., Orcutt, J.A., Harding, A.J., Kappus, M.E., Brocher, T.M., 1990. The structure of 0- to 0.2-my-old oceanic crust at 9 N on the East Pacific Rise from expanded spread profiles. J. Geophys. Res. 95, 15529–15556.
Wedepohl, K.H., 1995. The composition of the continental crust. Geochim. Cosmochim. Acta 59, 1217–1232.
Wiedenbeck, M., Goswami, J.N., Roy, A.B., 1996. Stabilization of the Aravalli Craton of northwestern India at 2.5 Ga: an ion microprobe zircon study. Chem. Geol. 129, 325–340.
Wilson, J.F., Nesbitt, R.W., Fanning, C.M., 1995. Zircon geochronology of Archaean felsic sequences in the Zimbabwe craton: a revision of greenstone stratigraphy and a model for crustal growth. In: Coward, M.E. (Ed.), Early Precambrian Processes, vol. Special Publication 95. Geological Society of London, London, UK, pp. 109–126.
Wyman, D., Kerrich, R., 2009. Plume and arc magmatism in the Abitibi subprovince: implications for the origin of Archean continental lithospheric mantle. Precambrian Res. 168, 4–22.
Youssof, M., Thybo, H., Artemieva, I.M., Levander, A., 2013. Moho depth and crustal composition in southern Africa. Tectonophysics 609, 267–287 (in this volume).
Zegers, T.E., van Keken, P.E., 2001. Middle Archean continent formation by crustal delamination. Geology 29, 1083–1086.
Zeh, A., Gerdes, A., Barton, J.M., 2009. Archean accretion and crustal evolution of the Kalahari Craton—the zircon age and Hf isotope record of granitic rocks from Barberton/Swaziland to the Francistown Arc. J. Petrol. 50, 933–966.
Zhang, S.B., Zheng, Y.F., Wu, Y.B., Zhao, Z.F., 2006. Zircon U–Pb age and Hf isotope evidence for 3.8 Ga crustal remnant and episodic reworking of Archean crust in South China. Earth Planet. Sci. Lett. 252, 56–71.
Zhao, G., Sun, M., Wilde, S.A., Sanzhong, L., 2005. Late Archean to Paleoproterozoic evolution of the North China Craton: key issues revisited. Precambrian Res. 136, 177–202.
Zheng, J.P., Griffin, W.L., O'Reilly, S.Y., Lu, F.X., Wang, C.Y., Zhang, M., Wang, F.Z., Li, H.M., 2004. 3.6 Ga lower crust in central China: new evidence on the assembly of the North China Craton. Geology 32, 229–232.
Zheng, J., Griffin, W.L., O'Reilly, S.Y., Zhang, M., Pearson, N., Pan, Y., 2006. Widespread Archean basement beneath the Yangtze craton. Geology 34, 417–420.
Zheng, T., Chen, L., Zhao, L., Zhu, R., 2007. Crustal structure across the Yanshan belt at the northern margin of the North China Craton. Phys. Earth Planet. Inter. 161, 36–49.